6-2018

An Evaluation of Host Factors as Novel Therapeutic Targets During Influenza Infection Using RNA Technologies

Michael Ryan Haden Thompson
California State University - San Bernardino

AN EVALUATION OF HOST FACTORS AS NOVEL THERAPEUTIC TARGETS DURING INFLUENZA INFECTION USING RNA TECHNOLOGIES

A Thesis

Presented to the

Faculty of

California State University,

San Bernardino

In Partial Fulfillment

of the Requirements for the Degree

Master of Science

in

Biology

---

by

Michael Ryan Haden Thompson

June 2018

AN EVALUATION OF HOST FACTORS AS NOVEL THERAPEUTIC TARGETS DURING INFLUENZA INFECTION USING RNA TECHNOLOGIES

A Thesis

Presented to the

Faculty of

California State University,

San Bernardino

By

Michael Ryan Haden Thompson

June 2018

Approved by:

Dr. Laura L Newcomb, Committee Chair, Biology

Dr. Nicole Bournias-Vardiabasis, Committee Member

Dr. Daniel Nickerson, Committee Member

ABSTRACT

Influenza A is a single-stranded, multi-segmented, negative sense RNA virus of the family Orthomyxoviridae and is the causative agent of seasonal Influenza. Influenza viruses cause significant impacts on a global scale with regard to public health and economics. Annual influenza virus infections in the United States account for over 200,000 hospitalizations, up to 49,000 deaths (cdc.gov), and an economic burden of $87.1 billion (Molinari, et al., 2007). Influenza A virus has caused several pandemics since the turn of the 20th century. The effects of Influenza on public health and economics, compounded with low efficacy of the annual vaccine and emerging antiviral resistance, brings to light the need for an effort to stem these impacts, prevent pandemics, and protect public health by developing novel treatments.

This project proposes an alternative approach to combatting Influenza by targeting crucial host factors hijacked during infection that, if inhibited, significantly impair viral RNA expression, but result in low toxicity to the host. The host factors we examined include RNA export factors (XpoT and Xpo5) and RNA helicases (UAP56 and URH49). We selected the paralogs URH49 (DDX39A) and UAP56 (DDX39B) because previous studies suggest differing roles during Influenza infection, but we theorize that their high degree of sequence similarity, similar function, and association with many of the same cellular factors may allow them to substitute for one another if one is knocked down or inhibited.

CRISPR was considered as the primary method to evaluate the effect of knockout of these factors on viral RNA expression and host cell toxicity. CRISPR is an RNA guided mechanism for gene editing and was to be used to make null mutations in the targeted host genes. However, CRISPR proved to be a significant challenge and while we could not conclusively confirm whether the CRISPR plasmids were effective at targeting our genes of interest, our initial results were not promising and we did not pursue this approach further. As an alternative, host RNA export factors were evaluated using siRNA to knockdown the factor prior to influenza infection. RNA was then analyzed by reverse transcription quantitative polymerase chain reaction (RT-qPCR). The potential of inhibiting UAP56 or URH49 as a novel therapeutic target was determined using a visual assessment of cell death.

We found that siRNA-mediated knockdown of XpoT and Xpo5 did not have any impact on viral RNA synthesis early during infection. siRNA against UAP56 and DDX39 (targets both UAP56 and URH49) resulted in significant impairment in viral RNA synthesis, confirming previously established work suggesting that UAP56 and URH49 have important roles during infection. Importantly, these helicases play an interferon (IFN) independent role to enhance viral replication, as indicated by analysis in IFN deficient VERO cells. A viability assay relying on trypan blue exclusion did not yield trustworthy results, so a visual assessment of cell death was done. The visual assessment confirms previously-established observations that Nxf1 (mRNA export factor) siRNA

treatments result in a high degree of cell death, indicating the toxic nature of Nxf1 inhibition. Cells treated with UAP56 or DDX39 siRNAs demonstrated little to no additional toxicity compared to the non-target control, suggesting they can be inhibited to serve as antiviral targets.

ACKNOWLEDGEMENTS

Thanks to Dr. Laura Newcomb for her great mentorship, continual (and often infinite) patience, confidence, encouragement, and dedication to excellent teaching and research. I could not have asked for a better mentor for this program.

Thanks to Dr. Nicole Bournias-Vardiabasis for her continual encouragement and confidence in my cell culture technique. The opportunity to assist with her tissue culture class was an invaluable experience.

Thanks to Dr. Daniel Nickerson for strength and honor, teaching me to teach others more effectively, and believing in my abilities, even when the future of this research was uncertain. A thesis defense is always 50% celebration because it means that your mentors think that you are ready.

Thanks to the Department of Biology faculty and staff for their great support during my program, especially in pushing me to be a better student and their confidence in my capabilities as a candidate for a Master's degree.

Thanks to the Office of Student Research for their generous funding of my research and employing me a Peer Leader and Research Consultant, which taught me much about teaching and supporting undergraduates at CSUSB.

Thanks to God, who always finds a way to remind me that I am gifted, capable, creative, passionate, and loved.

DEDICATION

This thesis is dedicated to the wonderful people in my life who always hold me up, have surety that I will achieve great things, make me smile, and support me through the joys and hardships of life. To my mother: Cathy, who has always inspired me to strive for excellence. To my grandparents: Shirley, David, and Diane, who always remind me to reach for the stars and have sacrificed so much for my sake. To my late relatives: Evelyn, Julie, and Virginia, who I wish could see how far I have come. To my closest friends: the Atwoods, the Oylers, Greg Bergevin, Justin Hackitt, and Teresa Crider-Mullin, who have seen me at my lowest and my highest and remind me always that life is a journey. To my wonderful counselor, Linda Hibbs, who, through guidance and wisdom, has helped to carry me through one of the most difficult, yet rewarding, periods of my life.

I dedicate this thesis, also, to those who doubt themselves. Through hard work, dedication, relentless love for those closest to you, and unwavering faith, all things are possible. This thesis is a testament to that.

TABLE OF CONTENTS

LISTOF FIGURES

CHAPTER ONE

BACKGROUND AND SIGNIFICANCE

Societal Impacts of Influenza A Virus

Influenza viruses have a unique history and origin: as early as the 15th century in Italy, there was an epidemic which was attributed to an “influence of the stars.” The epidemic was, in fact, caused by what we now know to be Influenza virus. It was because of this very epidemic that the virus became known as Influenza, its name taken from the Italian word *influenza*, which means “influence”. However, that is not the only epidemic (or pandemic) that Influenza has caused in its long history. The first pandemic was recorded in 1580 and at least four other pandemics were recorded later in the 18th century. It was not until 1933 that Smith, Andrews, and Laidlaw were able to isolate Influenza A from ferrets; Influenza B was isolated by Francois in 1936 (cdc.gov).

In addition to the pandemics of the 18th century, Influenza A has also caused several pandemics since the turn of the 20th century, including the 1918 Spanish Flu, 1957 Asian Flu, 1968 Hong Kong Flu, and 2009 Swine Flu. The Spanish Flu pandemic was incredibly widespread and had a higher mortality rate than other strains, with 20-40% of the worldwide population becoming ill and an estimated 50 million dying from the virus or complications associated with infection. The Asian Flu pandemic proved to be a classic example of “second wave” infections that are common among pandemics; even when the worst

seemed to be over, the virus made a resurgence shortly afterward, targeting a different group among the population. The Hong Kong Flu pandemic was both not as widespread as the Asian Flu and had even lower mortality in the United States, because its arrival coinciding with school children's vacation time in December (less close contact because they were not at school together), and advancements in antibiotic development curbed the effects of secondary bacterial infection. The Swine Flu pandemic began in the Spring, which gave the CDC little time to develop a vaccine; for these reasons, estimates put the number of H1N1-related infections between April 2009 and April 2010 at 43 million to 89 million and over 12,000 H1N1-related deaths (cdc.gov, 2011).

Influenza epidemics and pandemics are associated with antigenic drift and antigenic shift, which are important concepts related to genetics and the mutability of genetic information. Epidemics are mainly associated with antigenic drift, where a point mutation in a gene segment coding for a surface protein causes a minor change in protein structure. These changes result in a virus that can escape neutralizing antibodies, resulting in incomplete protection. A classic example of antigenic drift influencing Influenza epidemics involves the transition of A/Wuhan/359/95 (H3N2), a relative to the 1968 Hong Kong H3N2 strain, into A/Sydney/5/97 (H3N2) during the 1997-1998 flu season. The A/Sydney strain, which was still very similar to A/Wuhan, had changed enough that the vaccine administered for the flu season had little effect and became the predominant strain during the following season (cdc.gov, 2016). Pandemics are mainly

associated with antigenic shift, a much more significant change in genetic makeup. In the case of Influenza, antigenic shift typically occurs when multiple viruses infect a cell and their segments shuffle (reassortment), resulting in viruses that can contain completely new segments encoding very different surface antigens. The 2009 Swine Flu is a recent example of a virus formed by gene segment shuffling that resulted in a novel H1N1 strain which caused a major pandemic. The pandemic began early in Spring when there was no vaccine available and was characterized by morbidity and mortality far above expected values for the time of year. A 2011 study estimated that pandemic H1N1 resulted in more than 60 million cases of illness in America, 270,000 hospitalizations, and 12,500 deaths. Since the virus antigen had not been seen in recent years, 90% of these hospitalizations and deaths occurred in individuals under the age of 65. The low incidence of hospitalization of individuals older than the age of 65 is most likely attributed to existing immunity when this antigen was previously circulating. Typical seasonal influenza, however, causes 90% of hospitalizations and deaths in individuals *over* the age of 65 (cdc.gov, 2016).

Influenza viruses cause significant impacts on a global scale with regard to public health and economics. Annual influenza virus infections in the United States account for over 200,000 hospitalizations, up to 49,000 deaths (cdc.gov, 2016), and an economic burden of $87.1 billion (Molinari, et al., 2007). Worldwide, influenza virus infections result in 3-5 million cases of severe illness and 290,000-650,00 deaths annually (who.int). Therefore, it is pertinent that an

effort be put forth to stem these impacts, prevent pandemics, and protect public health by developing novel influenza treatments.

Influenza A Virus Biology

Influenza A is a member of *Orthomyxoviridae*, whose other members include the clinically and economically relevant Influenza B, Influenza C, Thogoto, Quaranfil, and Infectious Salmon Anemia viruses (Hutchinson, 2013). Influenza A is an enveloped, negative-sense, single-stranded RNA virus with eight genome segments that code for at least 11 unique proteins. The genome of Influenza A is packaged as viral ribonucleoproteins (vRNPs) that consist of one heterotrimeric RNA-dependent RNA polymerase (RdRP: PA, PB1, and PB2) and multiple nucleoproteins (NP) bound to a single genome segment. The vRNPs are encapsidated by a matrix protein (M1) and enveloped by a membrane containing Hemagglutinin (HA), Neuraminidase (NA), and proton channels (M2). There are 18 distinct variants of HA, and 11 for NA (cdc.gov, 2017). The virus also expresses three other non-structural proteins that range in function from nuclear export (NS2/NEP) to anti-viral response subversion (NS1) and alveolar macrophage destruction (PB1-F2) (O'Neill et al., 1998; Hale et al., 2008; Coleman, 2007, respectively).

Infection by the virus begins by receptor-mediated endocytosis of the virion after the binding of HA to terminal sialic acid residues of glycoproteins on the surface of target cells, distinguishing between α-2,6- and α-2,3-linked

glycoproteins in humans and avian species, respectively. It is important to note, however, that α-2,3-linked glycoproteins exist in human lung epithelium, but only in the lower respiratory tract, which is generally inaccessible to avian-specific viruses. HA exists as a trimer with two regions of distinct structure, with the head region containing the binding domain for the sialic acid receptor. Host serine proteases facilitate cleavage of HA into HA1 and HA2, with HA1 containing frequently-changing antigen sites, while HA2 facilitates membrane fusion. The endocytic vesicle fuses with an acidified late endosome, resulting in changes to internal and external viral proteins: the change in pH results in destabilization of internal matrix protein-protein interactions (via passage of hydrogen ions through M2 ion channels) and conformational change in external HA2, causing uncoating of the genome, the viral envelope to fuse with the late endosome, and release the vRNPs into the cytoplasm (Bouvier, et al., 2008). Nuclear localization signals (NLS) direct the cell to translocate the vRNPs to the nucleus where transcription begins (Bouvier, 2008). While the RdRP is capable of

Transcription of viral mRNAs is not facilitated by the host RNA polymerase II because it is a DNA-dependent enzyme. Instead, the encoded viral RNA-dependent RNA polymerase performs this function, albeit in a very unique way. The viral polymerase is not capable of recruiting capping machinery, so instead it cleaves 5'-capped RNA fragments from nascent cellular mRNAs in a process called "cap snatching" (Hutchinson, 2013). Similarly, it cannot recruit Poly-A Polymerase, a crucial enzyme required for synthesis of the poly-A tail on host cell

transcripts. Instead of snatching poly-A tails, a poly-U (poly-uracil) tract is encoded in each of the viral genome segments. Stuttering over this poly-U tract is the mechanism by which the virus synthesizes its poly-A tail (Bouvier, 2008). After cap snatching and poly-adenylating, viral mRNAs are exported to the cytoplasm. The HA, NA, and M2 envelope proteins are synthesized and sorted by membrane-bound ribosomes and trafficked to the plasma membrane (Bouvier, 2008). The polymerase subunits (PA, PB1, PB2) and NP are crucial for vRNP formation in the nucleus, but they are synthesized in the cytoplasm; the virus circumvents this problem by having an NLS on each subunit, which allows for interaction with importins. PA and PB1 are imported as a dimer while PB2 and NP are imported as separate monomers. These importins are also hypothesized to function as chaperones for PB1 and NP during assembly of the vRNP (Hutchinson, 2013).

During the course of infection, the multifunctional non-structural protein NS1 (with proposed dimerization states) serves a plethora of functions, including control of viral mRNA splicing, enhancement of viral mRNA translation, host immune response suppression, and strain-dependent pathogenesis (for review of NS1 function see Hale, 2008).

NS2, also known as Nuclear Export Protein (NEP), was once thought to be just a mere export protein. In reality, like its NS1 counterpart, it is quite multifunctional. Early studies implicated NS2 in the export of vRNPs during replication, but other studies have implicated it in regulation of viral mRNA and

antigenomic cRNA (an intermediate RNA used as a template for genome segment synthesis), adaptation of H5N1 (avian flu) in mammalian hosts, and release of budding virions from the host cell. NS2 is also highly conserved across all sequenced Influenza A strains with overall 93.4% amino acid identity and 96.3% C-terminal α-helix amino acid identity. NS2 interacts with Crm1 and its cofactor, RanGTP, through its NES to facilitate export of vRNPs. When Crm1 binds, it is believed that RanGTP binds to a separate yet unknown site on NS2. Although there is support for NS2 co-localizing with the vRNP during export, some argue that it not a central factor in the process. Regardless, a potential role for NS2 as a vRNP export factor cannot be easily dismissed (Paterson, 2012).

Once the vRNPs are exported to the cytoplasm, they are packaged into a new virion and exit through budding of the plasma membrane. Once the virus has budded from the cell, HA continues to anchor it to the cell surface due to its sialic acid binding activity. Neuraminidase (NA) exists as a mushroom-shaped tetramer that targets terminal sialic acid residues of glycoproteins and gangliosides. Its cleavage activity serves two purposes: (1) to release the new virus particles from the cell surface and (2) prevent virus particle aggregation by cleaving these residues on the surface of the viral envelope, enhancing infectivity (Bouvier, et al., 2008).

Current Treatments and Preventative Measures

The only current preventative measure against influenza virus infection is the trivalent or tetravalent annual vaccine. The composition of the vaccine depends on which strains are believed to be most prominent during the next flu season (cdc.gov, 2017). Although vaccination has revolutionized healthcare and the prevention of debilitating diseases such as polio and smallpox, there is yet to be a universal vaccine identified to protect against all subtypes of influenza and annual vaccination is required. Producing an annual vaccine on a large scale takes about six months of preparation; production needs to begin in March (and sometimes as early as January), so that the vaccine will be available by October (cdc.gov, 2017). Vaccination, overall, will never cease to be a valuable source of protection against infection, but there are several evident shortcomings to the annual flu vaccine, specifically, that affect its reliability to provide protection. The long period of time required to produce a vaccine means that they are of little use in an emerging viral pandemic. Additionally, records starting in 2004 show an 40% average efficacy of the vaccine to protect, but the 2014-2015 flu vaccine only had 19% efficacy due to antigenic drift of circulating strains during the course of vaccine development, leaving the vaccine less effective (cdc.gov, 2018). Vaccine protection also relies upon the immune system to recognize antigens and elicit a response specifically to them; if an individual suffers from an immune deficiency or they are genetically predisposed to having poor recognition of antigens, immunity may not be conferred. For all vaccines, our own genetics

and health history have a significant impact on the protective capabilities of the vaccine. However, in the case of influenza virus, the genetic variation in the virus over time has a significant impact in the protective capability of the vaccine, which makes it a protective measure that has variable efficacy year to year. Since annual vaccination is not enough to protect against influenza virus, antiviral treatments are required to stop viral spread.

Several antiviral drugs specific to influenza have been developed over the last 50 years. Amantadine and Rimantadine, whose mechanism of action involves blockage of the viral M2 ion channel, were the first generation of drugs used to treat influenza virus infection. Another class of drugs, which includes Oseltamivir, Zanamivir, and Peramivir, specifically inhibit cleavage of sialic acid by Neuraminidase and prevent virus release from the cell (cdc.gov, 2018).

Antiviral resistance has already been observed in strains of Influenza. According to the CDC, resistance to the adamantane class of drugs (Amantadine and Rimantadine) is widespread amongst all Influenza strains and 1.6% of H1N1 strains during the 2014-2015 flu season were resistant to Oseltamivir and Peramivir, meaning the genes encoding resistance are already circulating (cdc.gov, 2018). Although resistance to Neuraminidase inhibitors has not been observed in other influenza virus strains, the fact remains that resistance is a problem that will eventually lead to these drugs becoming useless.

One way in which viruses in general achieve drug resistance is through rapid evolution due to the short replication time; influenza virus can produce

1,000–10,000 particles per infected host in as little as 16 hours (Harvard Bionumbers, 2010). Additionally, administration of drugs creates an environment selective for resistant viruses. For examples, the DNA-dependent RNA polymerase of Human Immunodeficiency Virus (HIV) has low fidelity, accelerating the evolution of the virus when under selective pressure. A cocktail of drugs to treat the virus are effective for a period of time, but viral replication is so fast and produces so many varied viruses, termed quasi-species, that resistance can emerge before the virus can be cleared from the body. In light of antiviral drug resistance and the unreliable nature of the yearly influenza vaccine to protect against infection, an alternative approach must be considered that could potentially circumvent both these shortcomings.

An Alternative Approach to Combat Influenza

A universal truth related to all viruses is that they require a permissive host cell for replication. Some viruses, such Polyomaviruses, require the host to be mitotically active so they can access the nucleus and hijack the replicative machinery. Others, such as Hepatitis viruses, have liver cell-specific promotor sequences (targeted by liver-specific transcription factors) that only allow them to replicate within hepatocytes. In both of these examples, the viruses need to hijack cellular machinery to transcribe their genes and replicate their genome. Inhibition of cellular factors as opposed to viral targets is an alternative approach to inhibit viral infection. The major advantage to inhibiting hijacked host proteins

instead of viral proteins is that mutation of the drug target cannot occur during infection, decreasing the likelihood of selection for antiviral resistance. However, if the host target is essential, this could result in harm to the host cell. Still, cells often have multiple redundant proteins to provide similar function. In this alternative approach, we aim to identify a host factor which plays a redundant role in the host cell but an essential role in viral replication, thereby providing a useful host target to inhibit viral infection. We are interested in examining host RNA processing and export factors to determine if any can be targeted to inhibit influenza.

UAP56, URH49, and the DEAD-box Family of Helicases

Helicases as a whole act across a general or specific set of substrates and have a diverse array of functions, including separation of duplexes, regulated binding to single- or double-stranded DNA or RNA, remodeling of complex structures in RNA or RNA-protein complexes, and chaperoning self-splicing elements of mRNAs to within proximity of each other. The general mechanism of activity is by binding to a single strand and separating duplexes by translocating in a 3'→5' direction by ATP hydrolysis. Most helicases have a high degree processivity, meaning that the probability of the helicase remaining associated and continuing its activity after a successful cycle of ATP hydrolysis, translocation, and strand separation is high. For many helicases, they are capable of translocating hundreds or thousands of base pairs before dissociating.

DEAD-box helicases, however, have demonstrated poor helicase activity. Their effectiveness decreases substantially when they need to separate more than 10-15 base pairs at a time, but this is of little consequence with the consideration that RNA rarely has helices longer than 10 base pairs or so (Jarmoskaite, 2011).

The DEAD-box RNA helicase family of proteins, which include USP56 and URH49, is characterized by the Asp-Glu-Ala-Asp (D-E-A-D) motif common to this group. The local RNA remodeling activity of DEAD-box helicases makes them distinct from other groups of helicases, especially when only small select sections of an RNA need to be remodeled, as opposed to the global structure. UAP56 and URH49 function as pre-mRNA splicing factors and are crucial components of export complexes. UAP56 aids in the hTREX complex (couples transcription elongation to nuclear export) while URH49 aids in the hAREX complex (alternative RNA export) (Yamazaki, 2010). Both helicases have CRM1-independent nucleocytoplasmic shuttling activity and interact with REF, an established spliced- and unspliced-RNA export factor (Thomas, et al., 2011). UAP56 has also been shown to be essential in the function of the $U2AF^{65}$ splicing complex, specifically in the interaction with the branch point adenine, the nucleotide responsible for the nucleophilic attack that forms the lariat structure in group II introns (Fleckner, et al., 1997). As a whole, these helicases have redundant functions in the host cell, but essential functions in Influenza virus infection, making them potential novel antiviral targets. I am interested in

determining if UAP56, URH49, or both function as NP chaperones during influenza virus infection and can serve as useful antiviral targets.

. Previous research has implicated UAP56 as a hijacked host protein during Influenza infection. UAP56 was shown to associate with free NP and promote viral RNA synthesis *in vitro* (Momose, et al., 2001) by chaperoning NP onto the viral RNA during replication (Kawaguchi, et al., 2011). This function of UAP56 as a facilitator for viral RNA synthesis was also observed after eliminating its helicase through a targeted R365Q mutation, suggesting that its helicase activity is not required for its function in Influenza infection (Momose, et al., 2001). A paper by Wisskirchen in 2011 implicated UAP56, as well as its paralog URH49, in Influenza infection by their association with NP. Although UAP56 and URH49 share over 90% protein identify, the authors found only UAP56 was involved in the downregulation of dsRNA products during viral infection. These studies highlight several ways UAP56 and URH49 may be used to subvert the host cell and facilitate viral activity; more importantly, it suggests the two paralogs may maintain varied functions during viral infection.

RNA Export Factors: Nxf1, Crm1, XpoT, and Xpo5

RNA export from the nucleus is an essential function of cells. There are different export factors for different kinds of RNA; specifically, Nxf1 (mRNA), Crm1 (rRNA), XpoT (tRNA) and Xpo5 (miRNA). In the case of Influenza A, Nxf1 is implicated in some but not all influenza mRNA nuclear export (Larsen et al,

2014) while Crm1 is not involved in influenza mRNA nuclear export but is required for vRNP export during virion assembly (Elton et al, 2001). Inhibition of either will inhibit viral infection, but is also detrimental to the host cell. Given not all influenza mRNAs export via Nxf1, we aimed to decipher the importance of XpoT and Xpo5 for influenza infection.

In the cell, there are two main pathways through which mRNAs can exit the nucleus: usage of the Nxf1-Nxt1/Tap-p15 heterodimer or Crm1/Xpo1. Nxf1 is unique in that it has an RNA-binding domain, but it normally maintains a closed conformation, which makes it inefficient in binding RNA on its own. When the Transcription-Export Complex 1 (TREX1) is recruited to mRNA (in a splicing-dependent manner in humans), Nxf1 binds to TREX and a set of three SR proteins, adopting an open conformation and becoming able to efficiently bind RNA. The function of Nxt1 is still under investigation, but what is understood is that it stimulates binding of the Nxf1-RNA complex to nucleoporin p69. RNA is exported with the help of Dpb5 and Gle1 on the cytoplasmic side (for review see Carmody, 2009).

Crm1 cannot bind RNA directly. Instead, it relies on adaptor proteins in order to execute its functions. Crm1 interacts with many Ran-family proteins, including Ran-BP3 (binds RNA) and Ran-GTP. Through the interaction of these Ran proteins with the nuclear pore complex, mRNA is translocated to the cytoplasm (for review see Okamura, 2015). Crm1 is also involved in export of rRNA to the cytoplasm (Carmody, 2009).

XpoT (Los1 in yeast) is the principle factor involved in export of tRNA in vertebrates. Work in yeast with los1Δ strains shows an accumulation of processed, intron-containing tRNAs; the absence of splicing is due to the tRNA-specific splicing machinery existing on the outer mitochondrial membrane. Interestingly, los1Δ strains are viable, the *A. thaliana* XpoT homolog is nonessential, and insects lack an XpoT homolog but still manage to export tRNA, which suggests an additional novel export factor for tRNA. Xpo5 has been identified as an export factor for tRNA in *Drosophila* and yeast, but vertebrate Xpo5 is the principle factor in miRNA transport, so its role in tRNA export in humans is considered to be minor at best (Okamura, 2015).

Although Xpo5 exports tRNA in *Drosophila* and yeast, its primary function is to export miRNAs, small RNAs that are used for post-transcriptional regulation of gene expression. Mature miRNAs are synthesized as pri-miRNA (primary miRNA) by RNA polymerase II (RNAPII) and contain a local hairpin structure. Although RNAPII is classically associated with cellular mRNAs, pri-miRNAs are, in fact, 5'-capped and polyadenylated. Processing begins in the nucleus and ends in the cytoplasm. The canonical processing pathway involves Drosha-DGCR8 in the nucleus and Dicer-Argonaute in the cytoplasm; Drosha-DGCR8-independent, Dicer-independent, and TUTase-dependent pathways also exist for miRNA processing, often times for very specific miRNA products (Okamura 2015).

Overall, though each export factor functions as a principle factor for each class of RNA (mRNA, rRNA, tRNA, and miRNA), there is also a significant amount of overlap in the roles each can play. This may make it possible to identify a viable host target for inhibition.

RNA Technology: RNAi, siRNA, and CRISPR

RNAi, short for RNA interference, is a natural process involving small (20-30 nucleotides) non-coding RNAs (ncRNAs) that are used to control gene expression. Originally discovered as a microRNA (miRNA) in C. elegans, research on RNAi has revealed that up to 5% of the human genome is dedicated to the production of these ncRNAs that regulate the expression of least 30% of our genes, including those involved in cellular proliferation, differentiation, and chromatin packaging. RNA technology based on RNAi, termed siRNA (small interfering RNA), activates RNAi pathways to downregulate gene expression, but the RNAs are synthetic and exogenously supplied (for review see Wilson, 2013).

For siRNA inhibition, double stranded siRNAs ~ 21-25 nucleotides with 2-base 3’ overhangs on either end are transfected into cells and processed in the cytoplasm to associate with the RISC complex. The complex contains Dicer, Argonaute, and additional RNA Binding Proteins. Argonaute binds the 5’ and 3’ ends of a single strand (guide strand) in the dsRNA and discards the other (passenger strand). The RISC complex binds ssRNA, looking for partial complementarity, at minimum. This results in translational inhibition and often is

followed by deadenylation and degradation of the target mRNA occurs. (Wilson, et al., 2013).

Another RNA technology, CRISPR, which stands for Clustered Regularly Interspaced Short Palindromic Repeats, was originally discovered in the 1980s in E. coli, but its function was elucidated only as recently as 2007 when researchers discovered that Streptococcus thermophilius was able to develop resistance to bacteriophage by incorporating a fragment of the phage genome into its CRISPR locus (Barrangou, et al., 2007). More recently, Mimivirus, a large virus of amoeba, was discovered to have a CRISPR-like system to defend it from virophages (Levasseur, et al., 2016). This system, specifically type II, utilizes Cas9, a protein with DNA-binding, RNA-binding, and endonuclease activities, and a guide RNA (gRNA) specific to the sequence being targeted. Cas9 recognizes the protospacer adjacent motif (PAM) sequence NGG and, upon recognition, allows the gRNA to invade the DNA strand and check for complementarity. If the DNA is complementary, then Cas9 causes a blunt-end cleavage upstream of the PAM sequence. Non-homologous end joining becomes active and, in the event CRISPR is targeting a gene, causes insertions or deletions at the target site, effectively disrupting the gene. Variants of Cas9 have been developed that change its activity to that of a nickase, which initiates the high-fidelity homology directed repair (HDR) pathway. With the addition of a repair template, a gene can be modified while simultaneously reducing off-target effects (Cong, et al., 2013).

Here, I employed both RNA technologies to examine the roll of host RNA processing and export factors on influenza replication. CRISPR was attempted with little success to generate knock out UAP56 and URH49 cell lines. Since CRISPR was not successful we also employed siRNAs to downregulate these RNA helicases and additional host nuclear export factors. RNAi routinely inhibited target gene and we discuss the effects on viral RNA replication.

CHAPTER TWO

MATERIALS AND METHODS

Cells

A549 (Human Lung Adenocarcinoma) and Vero (African Green Monkey Kidney) were purchased from ATCC and cultured in the following conditions: 37^{o}C, 5% CO_2 in DMEM with 10% FBS (fetal bovine serum).

CRISPR Plasmids

Plasmids encoding CRISPR Cas9 and guide RNAs targeting UAP56 and URH49 (five for each gene) were provided by Horizon Discovery. Guide RNA sequences are withheld as proprietary information. Plasmids were transformed to *E. coli* DH5α and purified by Qiagen plasmid miniprep kit per the manufacturer's protocol.

DNA Transfection Protocol

For preliminary screening of CRISPR plasmids, A549 cells were seeded into 6-well plates at $0.3x10^6$ cells/mL. Cells were transfected at 40-50% confluency with Mirus LT-1 transfection reagent and allowed to incubate with CRISPR plasmid for 72 hours. Cells were harvested for further analysis.

FACS

A549 cells seeded into T-25 flasks with approximately $1.76x10^5$ cells. Cells were transfected at approximately 40-50% confluency with a 2:1 ratio of Mirus LT-1 transfection reagent (µL) to CRISPR-encoding plasmid DNA (µg). Cells were allowed to incubate for 72 hours before harvest. GFP expression from eGFP plasmid was used to evaluate if transfection was successful.

Sorting GFP and CRISPR Expressing Cells – FACS

Cells were collected 72 hours post transfection and prepped for FACS at University of California, Riverside (UCR). Cells were collected by trypsinization and centrifuged at 300xg for 7.5 minutes at 4°C. Trypsin was removed and cells were washed in sort buffer. Cells were centrifuged again under the same conditions. Sort buffer was removed and cells were resuspended in sort buffer to achieve a maximum concentration of $8.0x10^6$ cells/mL. Cells were transported to UCR on ice and sorting was performed using FACS Aria with GFP expression as the means for identifying cells expressing CRISPR.

Composition of Buffer Used for Resuspension of CRISPR Cells Before Sorting

1x Phosphate Buffered Saline (Ca^{2+}/Mg^{2+}-free to reduce intracellular adhesion), 1mM EDTA, 25mM HEPES (pH 7.0), 1% inactivated fetal bovine serum. Sort buffer was sterilized using a 0.2µm filter.

Analysis with Surveyor Nuclease

Genomic DNA Extraction

CRISPR-treated GFP-positive cells were centrifuged at 300xg for 7.5 minutes at 4^{o}C and buffer was removed. Genomic DNA was extracted with Invitrogen PureLink Genomic DNA Mini Kit according to manufacturer's specifications.

PCR Amplification of Target Regions of UAP56 and URH49

Primers were ordered from Fisher Scientific for UAP56 and URH49 with the follow sequences:

UAP56 Forward: 5'-CTTTGCTGTTCCTCAATCCC-3'

UAP56 Reverse: 5'-AGCTTTAGCCTCCTCCAGAT-3'

URH49 Forward: 5'-CTGTGGGCACTTTCCAGTTA-3'

URH49 Reverse: 5'-GGAGGGTGTTCTGTCTGT-3'

The target region of UAP56 or URH49 was amplified in a 50µL reaction using 2X PCR master mix (Promega) and 15-20ng of genomic DNA. The program for amplification for 35 cycles was as follows:

1. Initial denaturation: 95^{o}C for 60 seconds
2. Denaturation: 95^{o}C for 30 seconds
3. Annealing: 55^{o}C for 40 seconds
4. Extension: 72^{o}C for 75 seconds
5. Final extension: 72^{o}C for 5 minutes

10μL of PCR product was run on a 1% agarose gel for 40 minutes at 120V to assess the success of the reaction.

Treatment with Surveyor Nuclease

10μL of each PCR reaction using genomic DNA from CRISPR-treated GFP-positive cells was mixed with 10μL of PCR reaction using genomic DNA from untreated cells. PCR products were denatured and allowed to re-anneal to form hybrid DNA strands using a thermocycler with the following program:

1. 95°C for 10 minutes
2. 95°C → 85°C, -2.0°C/sec ramp, hold for 1 minute
3. 85°C → 75°C, -3.0°C/sec ramp, hold for 1 minute
4. 75°C → 65°C, -3.0°C/sec ramp, hold for 1 minute
5. 65°C → 55°C, -3.0°C/sec ramp, hold for 1 minute
6. 55°C → 45°C, -3.0°C/sec ramp, hold for 1 minute
7. 45°C → 35°C, -3.0°C/sec ramp, hold for 1 minute
8. 35°C → 25°C, -3.0°C/sec ramp, hold for 1 minute
9. 25°C → 4°C, hold indefinitely

The 20μL volume of heteroduplex DNA was treated with Surveyor Nuclease from Integrated DNA Technologies according to their protocol. Treated DNA was run on a 1% agarose gel to observe cleavage events.

siRNAs

siRNA SMARTpools targeting Nxf1, Crm1, XpoT, Xpo5, UAP56, and DDX39 were purchased from Dharmacon. Cells were seeded at $0.3x10^6$ cells/mL into 6-well plates. Cells at 50%-70% confluency were transfected with 25nM siRNA for 48 hours using Dharmacon reagent according to manufacturer's protocol.

Influenza Infection, RNA Extraction, and Quantitative PCR

48 hours post transfection, cells were infected with Influenza virus at an MOI of 4 for 4 hours, or mock infected. Egg amplified influenza virus was prepared in serum-free media with 1µg/mL N-acetyltrypsin. Media was removed from cells prior to infection and virus suspension was allowed to attach to cells for 1 hour. Virus suspension was removed and DMEM with 2.5% FBS was added to the cells for 3 hours. Media was then removed, cells washed with Ca^{2+}/Mg^{2+}-free PBS, and cells were collected with a cell scraper.

RNA Extraction, Concentration, and Integrity

RNA was isolated using Trizol according to manufacturer's protocol. RNA concentration was determined using Nanodrop ND-1000 and a 1% agarose/1% bleach gel was made to assess the integrity and confirm concentration of the RNA. RNA was resolved on the gel at 120V for 1 hour.

Reverse Transcription

1000ng of RNA was used for reverse transcription with the AMV RT kit from Promega using oligo dT primer. Prior to reverse transcription, RNA was denatured at 70^{o}C for 10 minutes in a water bath. The 20µL reaction was performed at 42^{o}C in a water bath for 1 hour. The AMV RT enzyme was denatured at 95^{o}C for 5 minutes, then samples were allowed to cool on ice for 5 minutes. 80µL of 10mM Tris (pH 7.5) was then added to the cDNA.

Quantitative PCR

Quantitative PCR was performed using the StepOne Plus Real Time PCR system (Applied Biosystems) using SYBR Green master mix from Applied Biosystems or Agilent. Gene specific primers used were as follows:

NP Forward: 5'-GTGTGCAACCTGCATTTTCTGT-3'

NP Reverse: 5'-TCTGAGGTTCTTCCCTCCGTATT-3'

PA Forward: 5'-GGACAAATGGAACATCAAAGATTAAA-3'

PA Reverse: 5'-CAGAAGACTCGGCTTCAATCATG-3'

Nxf1 Forward: 5'-CATGAGCTACCCCCACCAAT-3'

Nxf1 Reverse: 5'-CCCTTGCAGGGCGGTAA-3'

Crm1 Forward: 5'-GATCCACAGATGGTCGCTGAA-3'

Crm1 Reverse: 5'-CTCTAGCAGCTGGGACATTTCTC-3'

XpoT Forward: 5'-AGATGTTCATGCCCCTGCTT-3'

XpoT Reverse: 5'-ACTCCTCCGCAACATCTGCTT-3'

Xpo5 Forward: 5'-CCATCTTTGAACCCTGAATCAAG-3'

Xpo5 Reverse: 5’-TAGAGATCGGCTACAAAGGGAAA-3’

UAP56 Forward: 5’-CAGACAGGCATTTTCCAAAGC-3’

UAP56 Reverse: 5’-CGCAAGGGACCGGAAAC-3’

URH49 Forward: 5’-GCTCCCCCTAAGAAAGACATCAA-3’

URH49 Reverse: 5’-TCCGGCTTCAGCAGAAAGTC-3’

Quantitative PCR Analysis

Data was collected as C_T values and analyzed using Microsoft Excel with the formula: $2^{(\text{CT average control sample} - \text{CT average treated sample})}$. All statistical analysis set $p \leq 0.05$ as significant. For samples with an equal number of data points, a two-tailed paired T-test was performed. Error bars were calculated using the standard deviation of data set divided by the square root of the number of samples.

Cell Viability

Cells for this assay were transfected with siRNA SMARTpools targeting Nxf1, UAP56, DDX39 sequences, and a non-target scramble. Cells were imaged and assessed visually before performing a trypan blue exclusion assay. Cell viability was assessed using Countess FL II from Invitrogen. 48 hours post transfection, cells were collected by cell scraping and suspended in 1mL of DMEM with 10% FBS. A 50µL aliquot of cells was taken for assessment of viability using 0.4% Trypan Blue. Cells were mixed 1:1 with Trypan Blue and loaded into BioRad cell counting slides.

CHAPTER THREE

CRISPR-MEDIATED KNOCKOUT OF UAP56 AND URH49

Background

We took advantage of Horizon Discovery's free offer to test potential CRISPR guide RNAs against cellular factors of interest. We selected two candidates, UAP56 and URH49, to investigate how the absence of these RNA helicases might impact viral RNA expression. Influenza primarily infects lung tissue, so we chose to use A549 cells because they represent the most appropriate cell model for influenza infection. Horizon Discovery provided 10 plasmids (5 different guide RNAs per gene target) encoding guide RNA, modified Cas9, and Dasher-GFP. These plasmids were used in transfection, according to the workflow shown in figure 1.

Transfection of CRISPR Plasmids

In addition to the CRISPR plasmids, which themselves encode GFP, we also transfected a separate sample of cells with eGFP, which allowed us to assess transfection efficiency separately. Transfection efficiency for eGFP was typically high, similar to the fluorescent microscopy image shown in figure 1. CRISPR plasmids typically had much lower transfection efficiencies, estimated to be less than 10%.

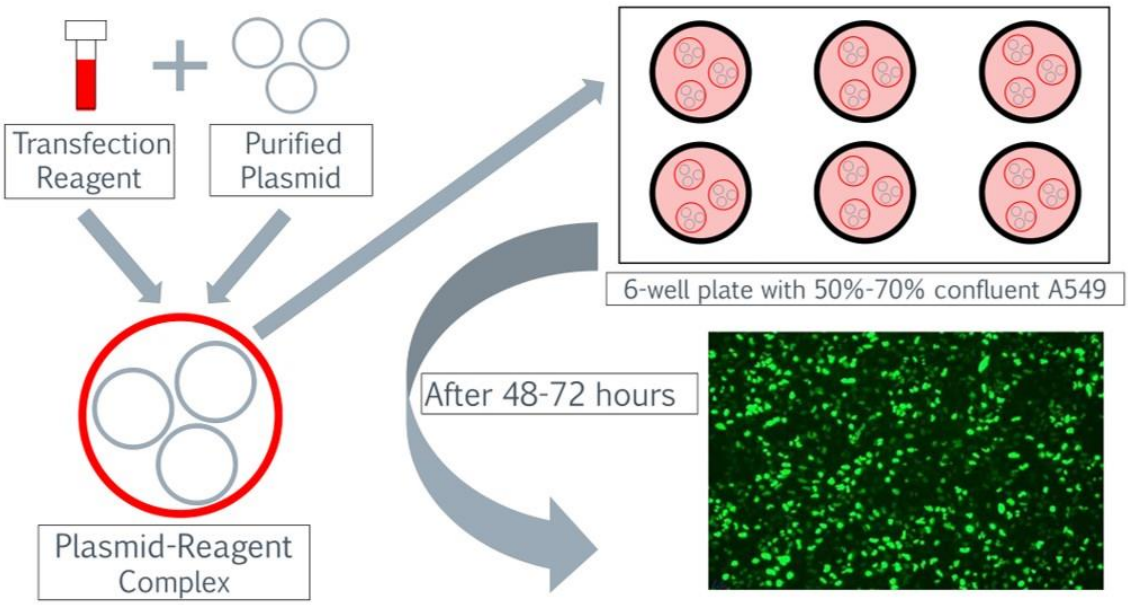

Figure 1 – *CRISPR plasmid transfection workflow* – A549 cells were seeded in a 6-well plate before transfection. Mirus LT-1 transfection reagent was complexed with CRISPR plasmid and allowed to incubate with cells for 48-72 hours before harvesting.

Initial Testing Using Surveyor Nuclease

Surveyor nuclease recognizes mismatched bases in double stranded DNA. We employed surveyor nuclease to assess whether the CRISPR plasmid guide RNAs were successful in targeting and creating null mutations in the target genes.

To demonstrate Surveyor nuclease function, two control DNA from the purchased kit were PCR amplified within a region which differed only in the presence of a C nucleotide or G nucleotide. PCR products of 600 base pairs were amplified, mixed, denatured, and then allowed to hybridize. The hybrid products were aliquoted into separate tubes and Surveyor nuclease was added. At the intervals of 10, 20, 30, 45, and 60 minutes, stopping solution was added to prevent further nuclease activity. The digested products were run on an agarose gel and the minimum time required to observe cleavage bands was determined (figure 2).

As control, the original PCR products were denatured and allowed to reanneal before incubation with surveyor nuclease for 60 minutes as a control for the enzyme's exonuclease activity which competes with its mismatch endonuclease activity. Magnesium in the reaction tends to bias the enzyme toward its endonuclease activity as well. A small amount of smearing beneath the control samples indicate very slight exonuclease activity, given there is some smearing observed in the no nuclease control. In the reaction samples, specific cleavage bands are visible by 30-minute incubation of the mismatch, indicating

that endonuclease activity is preferred. No significant banding can be observed at 10 and 20 minutes, but is clearly visible from 30 minutes onward, with no improvement of endonuclease activity by 60 minutes. Therefore, we determined two things: (1) that 30 minutes is the minimum time required to observe bands and (2) that 45 minutes is the time point where maximal cleavage is observed.

To assess CRISPR activity from the Horizon Discovery plasmids, DNA was extracted using the PureLink Genomic DNA mini kit from ThermoFisher. Genomic DNA, from both CRISPR-transfected cells and control cells, was used as a template in PCR to amplify both UAP56 and URH49 genomic DNA surrounding the CRISPR targeted region. PCR products from control and transfected cells were mixed together and denatured through heating. In a slow, step-by-step cooling process, the products re-anneal and if CRISPR worked, mismatches within the DNA duplex between control and CRISPR treated should produce a bubble at which Surveyor will cut. As a control, UAP56 PCR product and URH49 product were mixed, annealed and treated. In initial trials, no cleavage bands could be observed in PCR products amplified from cells transfected with any of the CRISPR plasmids. Given the low transfection efficiency, we reasoned most genomes remained intact and our PCR product would reflect this. Therefore, we decided to use Fluorescence Activated Cell Sorting (FACS) to select for the GFP-positive population which would yield a definitive answer to whether the Horizon Discovery designed plasmids targeted the intended genes of interest.

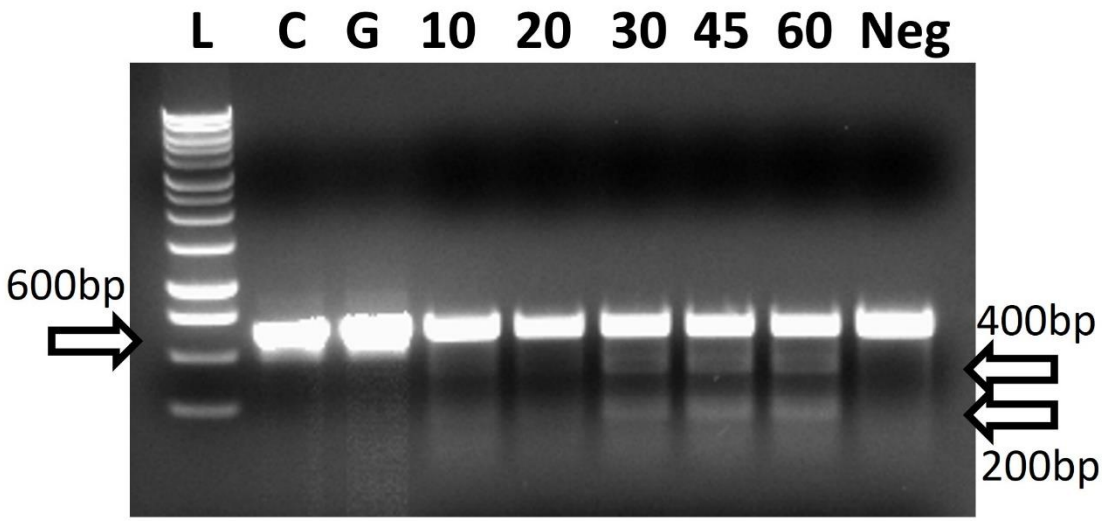

Figure 2 – *Surveyor nuclease control test with C and G plasmid* – lane 1: ladder; lane 2,3: pure control plasmid PCR product (600 base pairs) with no nuclease; lane 4-8: digest of hybridized control C and G products at 10, 20, 30, 45, and 60 minutes; lane 9: denatured and re-annealed control C PCR product only in the presence of Surveyor nuclease for 60 minutes. Surveyor cleavage products expected at 200 and 400 base pairs are observed by 30 minutes, but most prominently after 45 minutes.

Cell Sorting with FACS

Due to the low efficiency of transfection with the CRISPR plasmids in A549 cell, we sorted and collected GFP expressing cells to enrich for a population of cells with high levels of GFP expression, indicating the presence and expression of CRISPR plasmid. Cells were harvested by scraping, washed and suspended in a sorting buffer, and then transported on ice to the Institute for Integrative Genome Biology at University of California Riverside.

FACS analysis was performed using different comparisons of forward scatter and side scatter to eliminate cellular debris and cellular doublets from the final isolated population and estimation of transfection efficiency. In figures 3-12, panel A displays time vs. forward scatter and demonstrates the constant flow of the FACS machine. While nearly all candidates demonstrated a relatively constant flow during sorting, candidate 15 did not. Most of. Panel B demonstrates the comparison of forward scatter vs. side scatter and is used to exclude cellular debris from the isolated population. In the bottom left corner of the field, a high density of events with small size (low forward scatter) and low complexity (low side scatter) indicates the presence of cellular debris. For further analysis, these events were excluded using a gate (red outline around the large cluster of events). Panel C demonstrates the comparison of forward scatter area vs. forward scatter height. Height, during sorting, is the intensity of the forward scatter signal. The area is a product of the height and width of the signal (how long it takes the cell to move through the detector). When cells are stuck

together, they do not cause an increase in signal height, but increase the width. As a result, the area increases without an increase in height. This comparison, ultimately, allows us to exclude doublets and clumps of cells, some of which may express GFP some may not. The blue gate, drawn around the cluster of cells moving diagonally up and to the right, indicates single cells. Panel D demonstrates a Principal Component Analysis (PCA), a mathematical transformation which group like populations together for easier identification of the GFP-positive population of cells. The PCA used forward scatter and GFP expression to show events that displayed higher intensities of GFP in single cells. The percentage of GFP-positive single cells ranged from 0.9% to 4.1%, confirming low transfection efficiency with CRISPR plasmids. From this we were able to isolate genomic DNA from only $5x10^4$--$2.2x10^5$ cells.

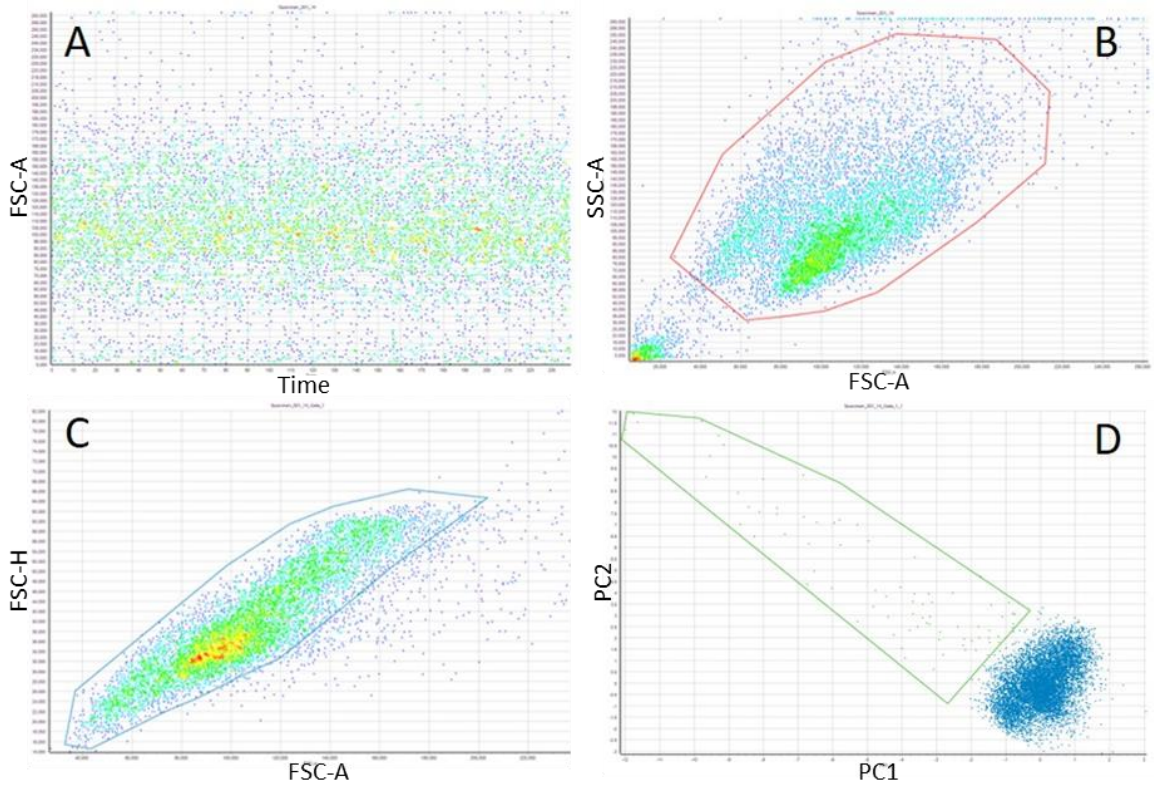

Figure 3 – *CRISPR plasmid candidate 14 (URH49) FACS analysis* – Panel A (time vs. FSC-A) Even distribution of events indicates that flow through FACS was constant. Panel B (FSC-A vs. SSC-A): Comparison of forward scatter and side scatter reveals two distinct populations of events. The lower corner is composed of cellular debris while the moderately dense region of events (green, light blue) within the gating are whole cells. Panel C (FSC-A vs. FSC-H): Doublet exclusion of events. Panel D (PCA of FSC-A vs. GFP): PCA revealed that 0.9% of cells were GFP-positive.

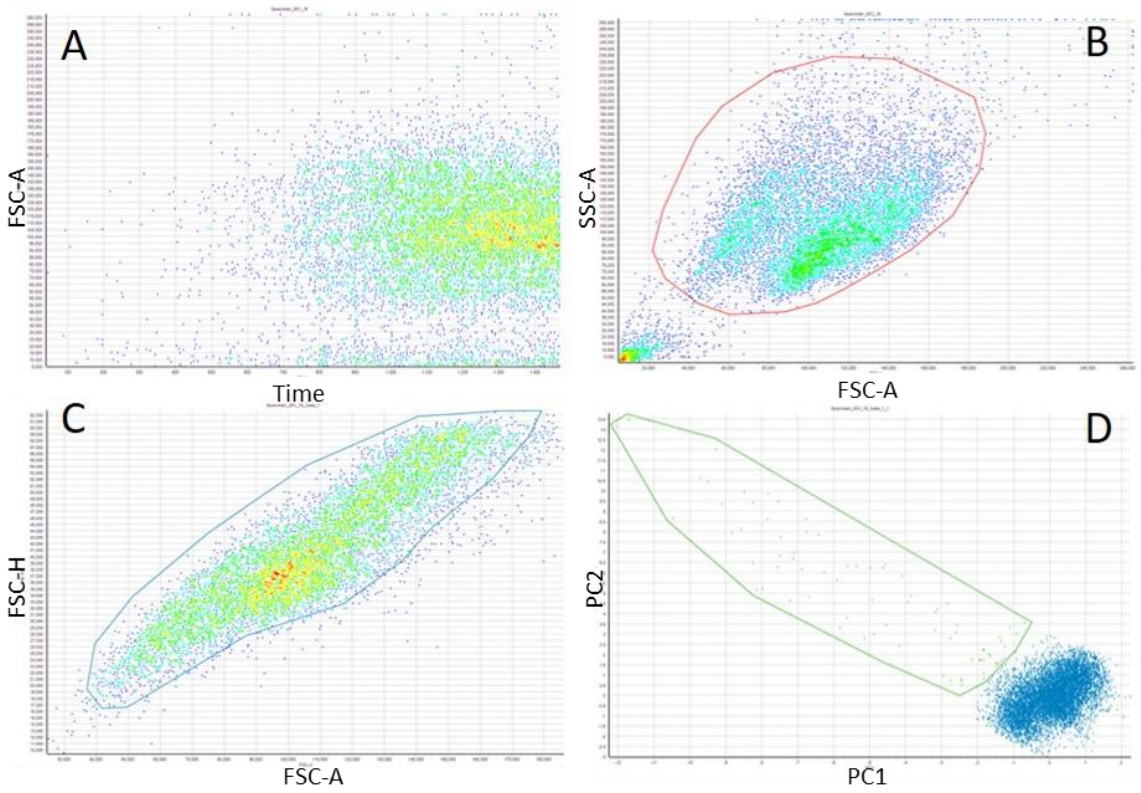

Figure 4 – *CRISPR plasmid candidate 15 (URH49) FACS analysis* – Panel A (time vs. FSC-A) Disruptions at the start of FACS create a delay in the sorting process. When sorting begins (approx. 700 seconds), the process in slowed to ensure that clogging did not occur. Panel B (FSC-A vs. SSC-A): Comparison of forward scatter and side scatter reveals two distinct populations of events. The gating around the large cluster of events indicates single cells. Panel C (FSC-A vs. FSC-H): Doublet exclusion of events. Panel D (PCA of FSC-A vs. GFP): PCA revealed that 0.9% of cells were GFP-positive.

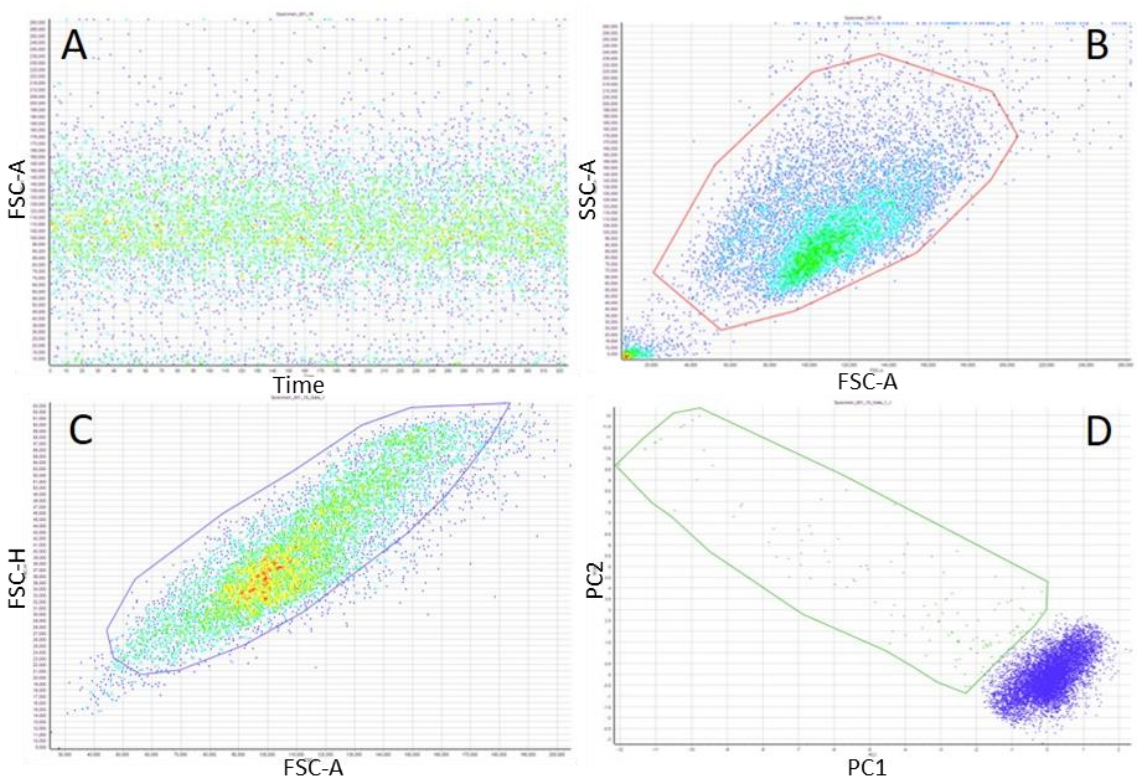

Figure 5 – *CRISPR plasmid candidate 16 (URH49) FACS analysis* – Panel A (time vs. FSC-A) Even distribution of events indicates that flow through FACS was constant. Panel B (FSC-A vs. SSC-A): Comparison of forward scatter and side scatter reveals two distinct populations of events. Cellular debris in the lower left corner is excluded from analysis. Panel C (FSC-A vs. FSC-H): Doublet exclusion of events. Panel D (PCA of FSC-A vs. GFP): PCA revealed that 1.4% of cells were GFP-positive.

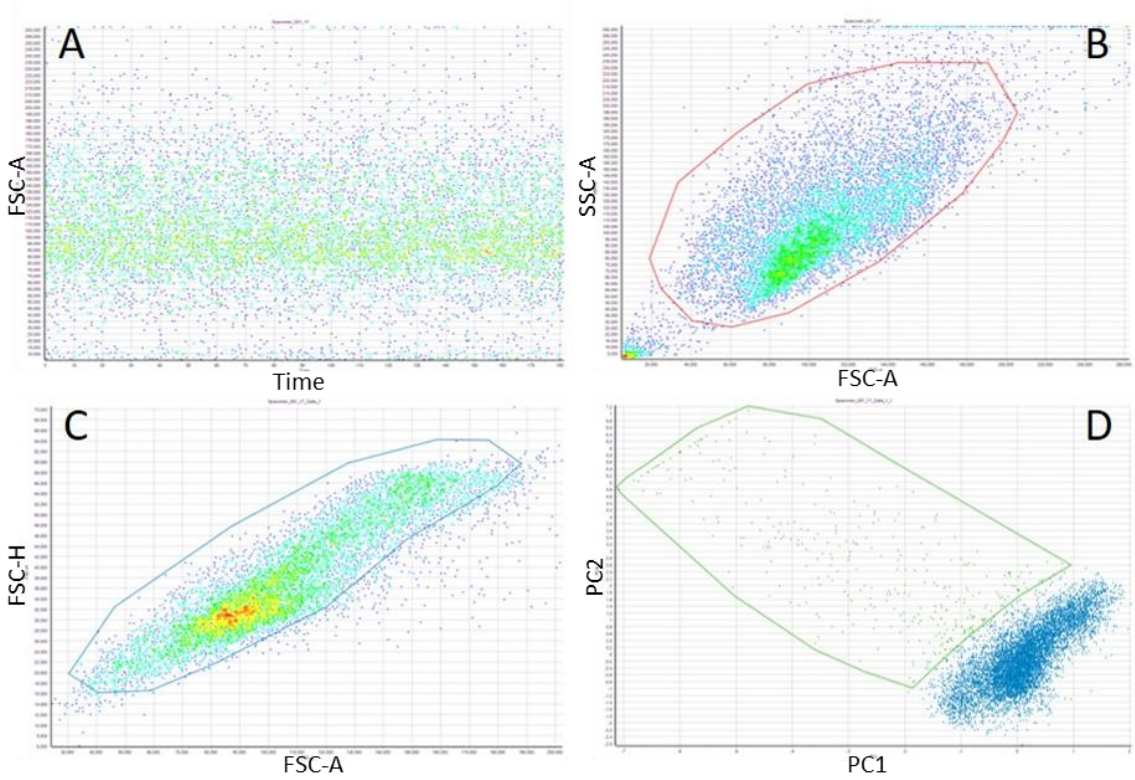

Figure 6 – *CRISPR plasmid candidate 17 (URH49) FACS analysis* – Panel A (time vs. FSC-A) Even distribution of events indicates that flow through FACS was constant. Panel B (FSC-A vs. SSC-A): Comparison of forward scatter and side scatter reveals two distinct populations of events. The lower corner is composed of cellular debris while other events within the gating are whole cells. Panel C (FSC-A vs. FSC-H): Doublet exclusion of events. Panel D (PCA of FSC-A vs. GFP): PCA revealed that 4.1% of cells were GFP-positive.

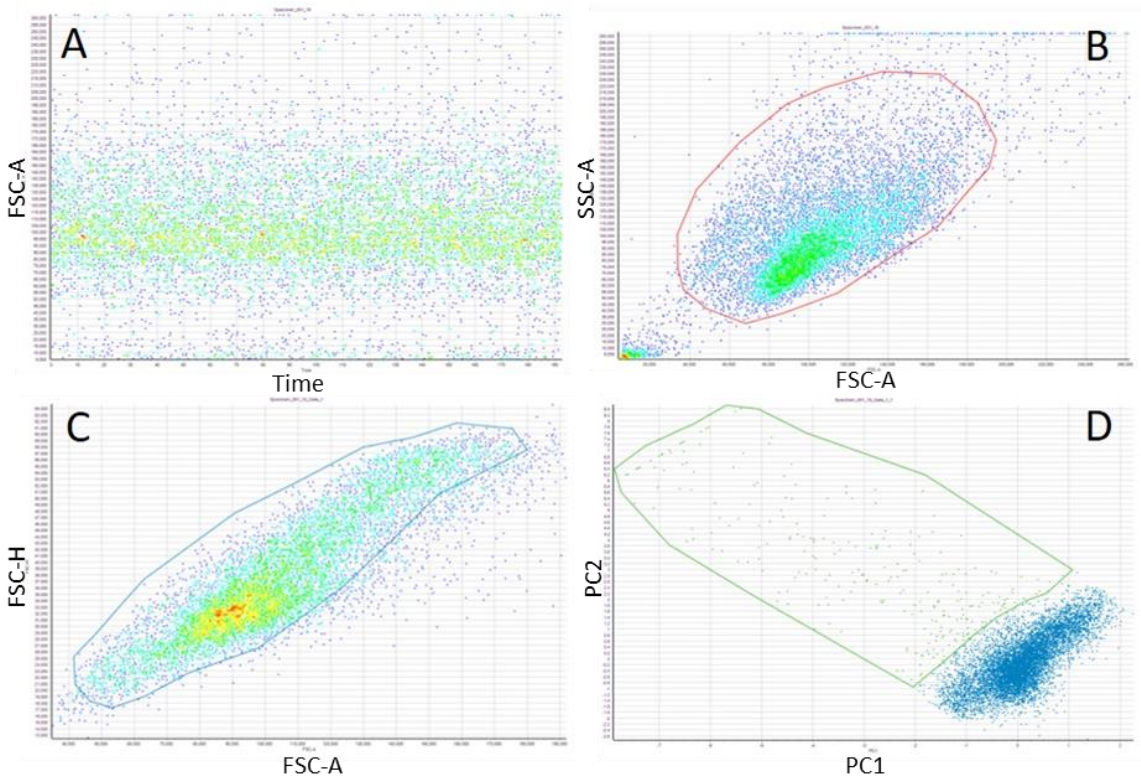

Figure 7 – *CRISPR plasmid candidate 18 (URH49) FACS analysis* – Panel A (time vs. FSC-A) Even distribution of events indicates that flow through FACS was constant. Panel B (FSC-A vs. SSC-A): Comparison of forward scatter and side scatter reveals two distinct populations of events. The lower corner is composed of cellular debris while other events within the gating are whole cells. Panel C (FSC-A vs. FSC-H): Doublet exclusion of events. Panel D (PCA of FSC-A vs. GFP): PCA revealed that 3.1% of cells were GFP-positive.

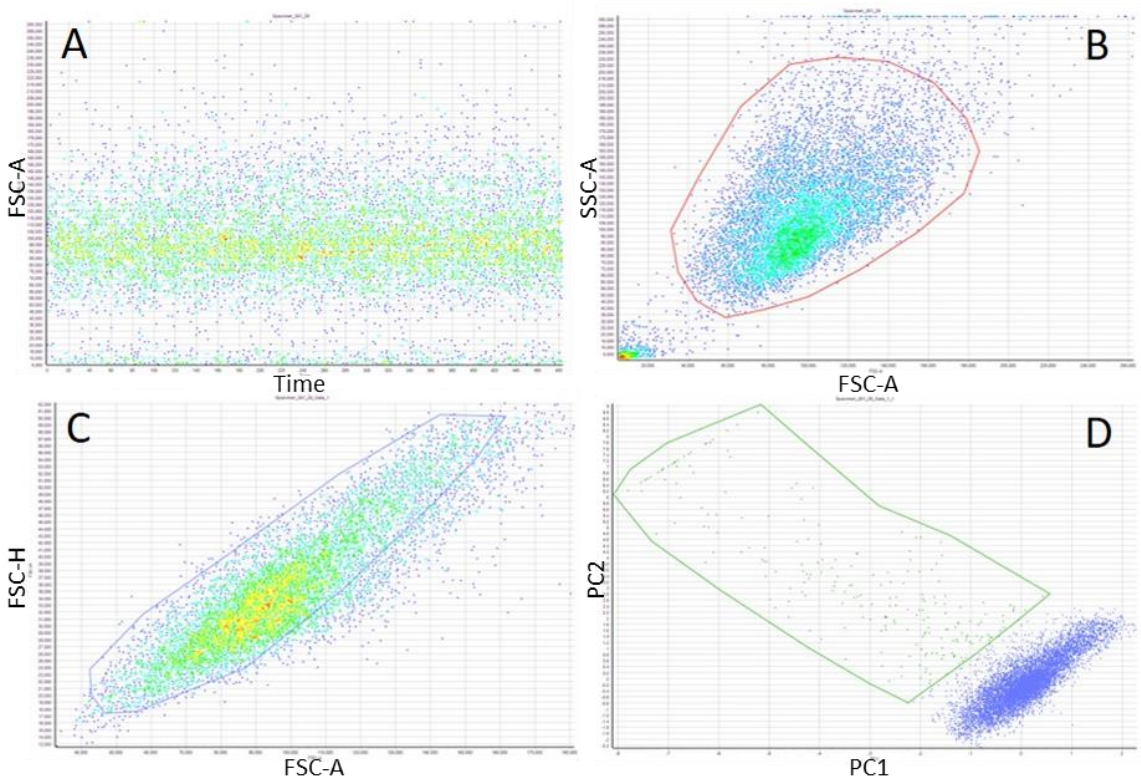

Figure 8 – *CRISPR plasmid candidate 29 (UAP56) FACS analysis* – Panel A (time vs. FSC-A) Even distribution of events indicates that flow through FACS was constant. Panel B (FSC-A vs. SSC-A): Comparison of forward scatter and side scatter reveals two distinct populations of events. The lower corner is composed of cellular debris while other events within the gating are whole cells. Panel C (FSC-A vs. FSC-H): Doublet exclusion of events. Panel D (PCA of FSC-A vs. GFP): PCA revealed that 2.2% of cells were GFP-positive.

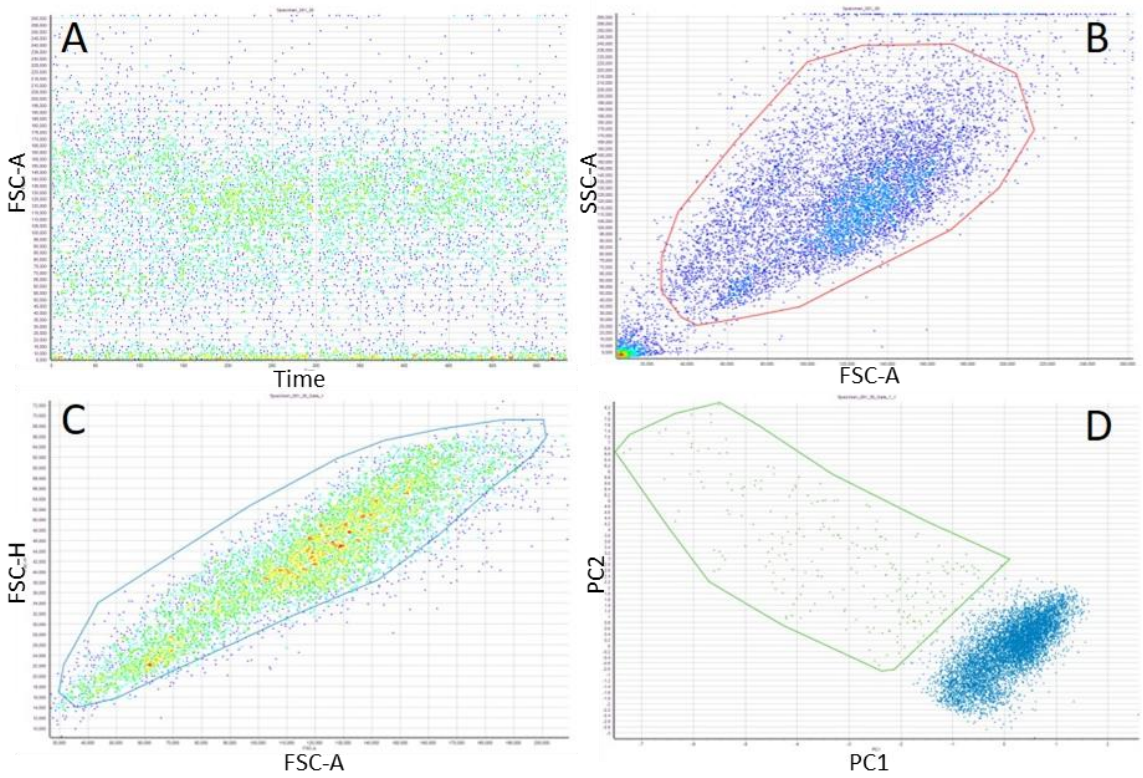

Figure 9 – *CRISPR plasmid candidate 30 (UAP56) FACS analysis* – Panel A (time vs. FSC-A) Even distribution of events indicates that flow through FACS was constant. Panel B (FSC-A vs. SSC-A): Comparison of forward scatter and side scatter reveals two distinct populations of events. The lower corner is composed of cellular debris while other events within the gating are whole cells. Panel C (FSC-A vs. FSC-H): Doublet exclusion of events. Panel D (PCA of FSC-A vs. GFP): PCA revealed that 3.1% of cells were GFP-positive.

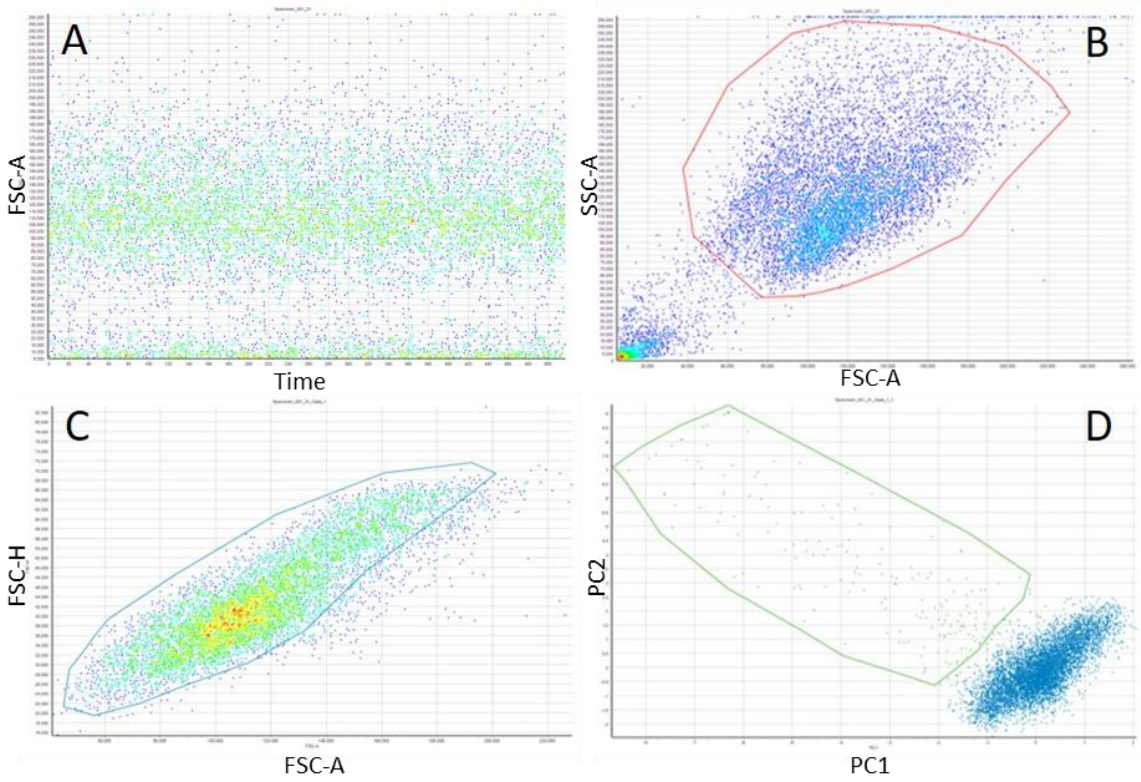

Figure 10 – *CRISPR plasmid candidate 31 (UAP56) FACS analysis* – Panel A (time vs. FSC-A) Even distribution of events indicates that flow through FACS was constant. Panel B (FSC-A vs. SSC-A): Comparison of forward scatter and side scatter reveals two distinct populations of events. The lower corner is composed of cellular debris while other events within the gating are whole cells. Panel C (FSC-A vs. FSC-H): Doublet exclusion of events. Panel D (PCA of FSC-A vs. GFP): PCA revealed that 2.4% of cells were GFP-positive.

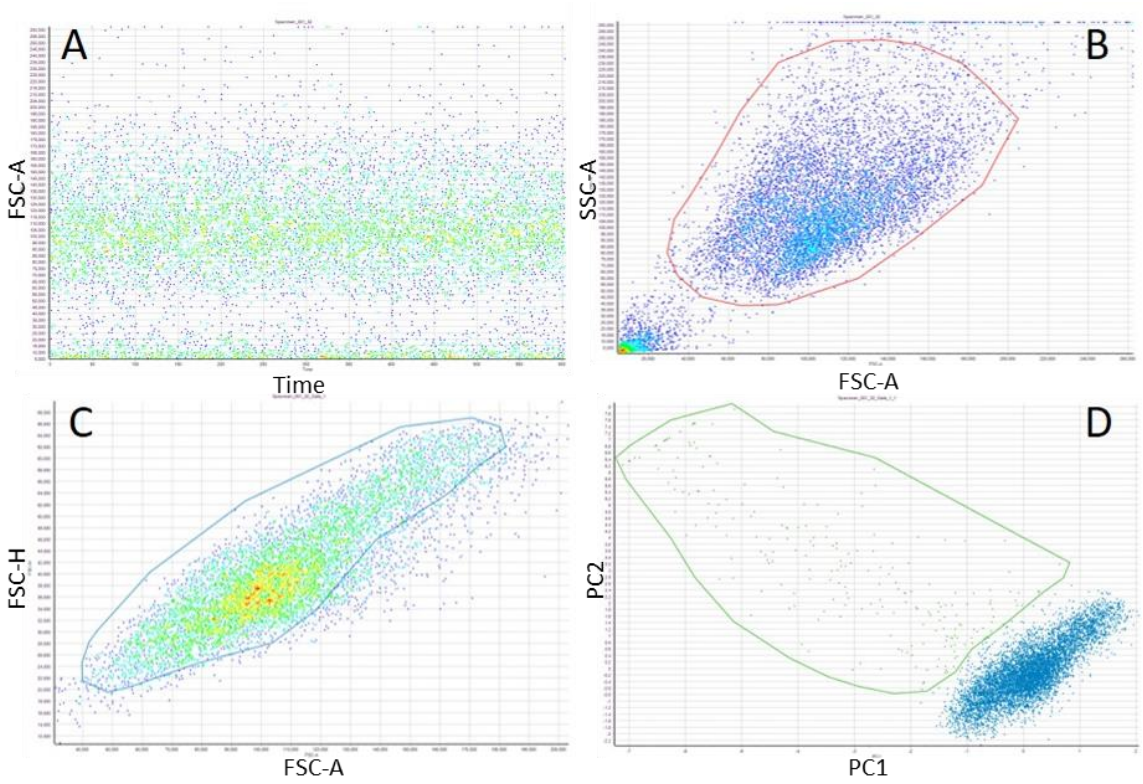

Figure 11 – *CRISPR plasmid candidate 32 (UAP56) FACS analysis* – Panel A (time vs. FSC-A) Even distribution of events indicates that flow through FACS was constant. Panel B (FSC-A vs. SSC-A): Comparison of forward scatter and side scatter reveals two distinct populations of events. The lower corner is composed of cellular debris while other events within the gating are whole cells. Panel C (FSC-A vs. FSC-H): Doublet exclusion of events. Panel D (PCA of FSC-A vs. GFP): PCA revealed that 3.2% of cells were GFP-positive.

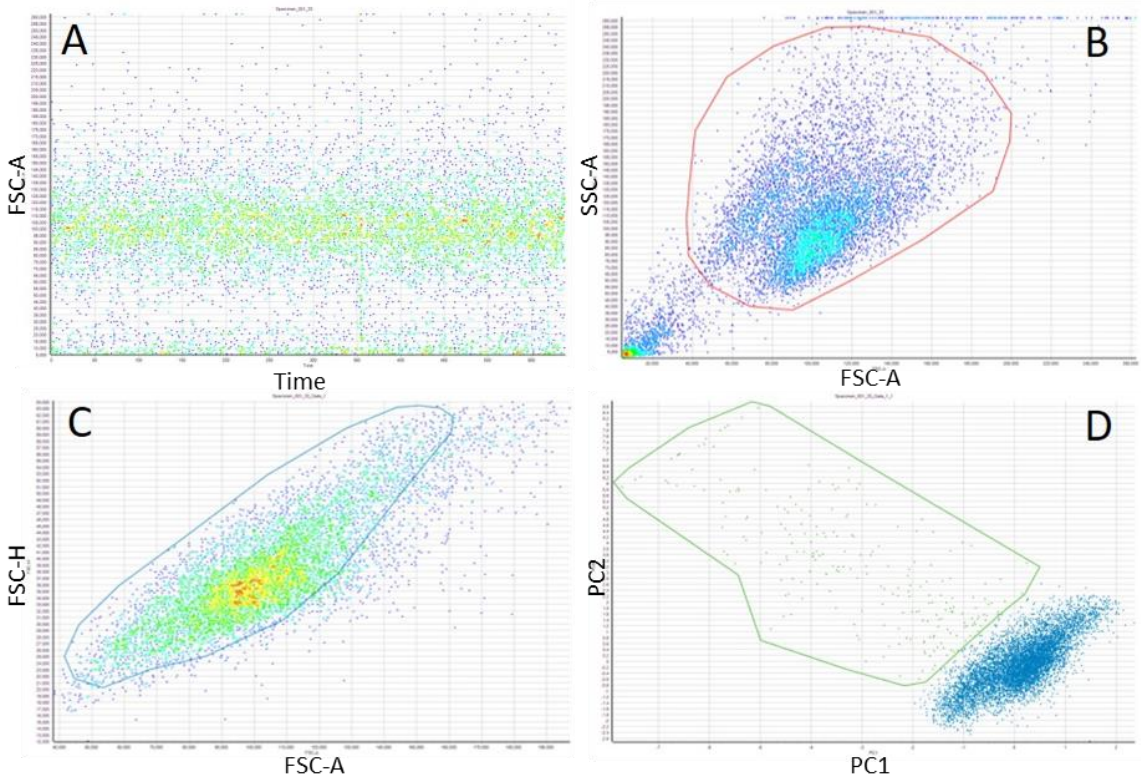

Figure 12 – *CRISPR plasmid candidate 33 (UAP56) FACS analysis* – Panel A (time vs. FSC-A) Even distribution of events indicates that flow through FACS was constant. Panel B (FSC-A vs. SSC-A): Comparison of forward scatter and side scatter reveals two distinct populations of events. The lower corner is composed of cellular debris while other events within the gating are whole cells. Panel C (FSC-A vs. FSC-H): Doublet exclusion of events. Panel D (PCA of FSC-A vs. GFP): PCA revealed that 3.2% of cells were GFP-positive.

Surveyor Nuclease Assay After FACS

Genomic DNA was extracted from the GFP-positive population of cells (less than 10ng/uL for all samples) and used in PCR for the Surveyor nuclease assay. In the first run (figure 13), URH49 did not amplify from the genomic DNA template while UAP56 amplified strongly, displaying bands at the predicted length of 1100 base pairs. URH49 primers had previously been tested and were shown to amplify from genomic DNA very well, also producing bands at 1100 base pairs, so this result was very unexpected.

A second attempt was made to amplify URH49 (figure 14). While UAP56 failed to amplify in just one sample in this trial, amplification of URH49 produced bands indicating non-specific products. Specific amplification of URH49 varied from very weak to moderately strong. At this point, there was not enough genomic DNA to continue assessing URH49 candidates, so an effort was made to assess UAP56 candidates.

UAP56 PCR products were analyzed using Surveyor nuclease (figure 15). The positive control with hybridized control C and G products did not appear to cut; making our results inconclusive. While we see banding at 600 base pairs in the UAP56 candidate lanes, indicative of nuclease activity, the size was unexpected for the predicted sizes expected to result from surveyor cleavage of the CRISPR directed gene edit and appeared instead to be indicative of the enzyme’s exonuclease activity. Surveyor has both endonuclease and exonuclease activity, but the buffer used for the assay tends to suppress

exonuclease activity while giving preference to the endonuclease activity. There was not enough genomic DNA to continue assessment of UAP56 candidates and given results were not promising, we did not pursue this approach further.

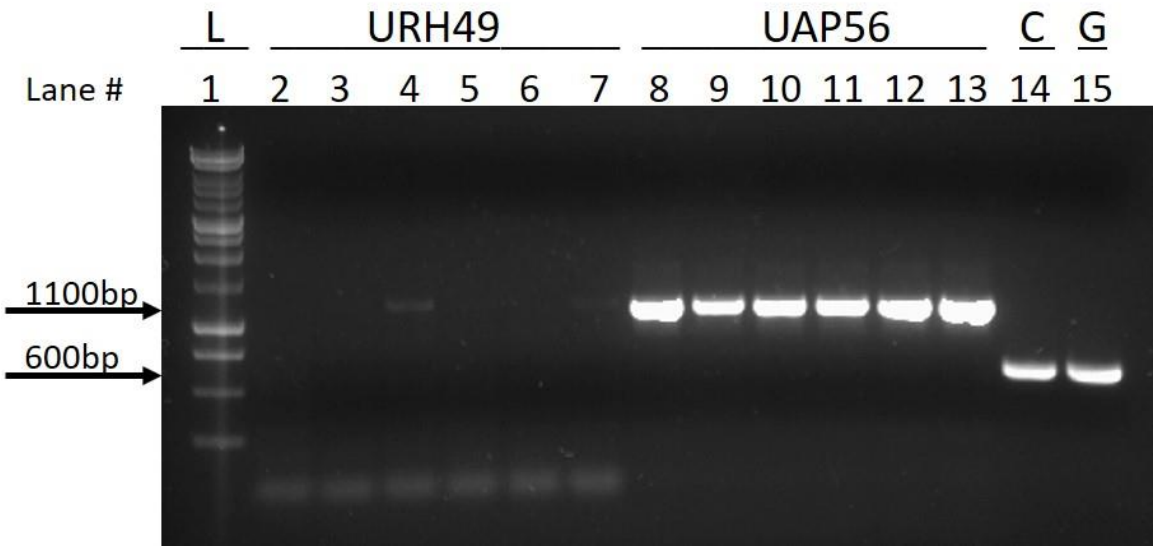

Figure 13 – *Amplification of URH49 and UAP56 from GFP-positive population obtained through FACS* – Lanes 2-6: URH49 candidates 14-18. Lane 7: Amplification of URH49 from untreated control cells. Lanes 8-12: UAP56 candidates 29-33. Lane 13: Amplification of UAP56 from untreated control cells. Lanes 14-15: Surveyor Control C and G. Amplification of URH49 and UAP56 sequences should produce a band at 1100 base pairs while Control C and G sequences should appear at 600 base pairs. URH49 sequences did not appear to be amplified while UAP56 sequences showed strong amplification. Control C and G were also successfully amplified. A second PCR, in an attempt to amplify URH49 sequences, was performed as a follow up.

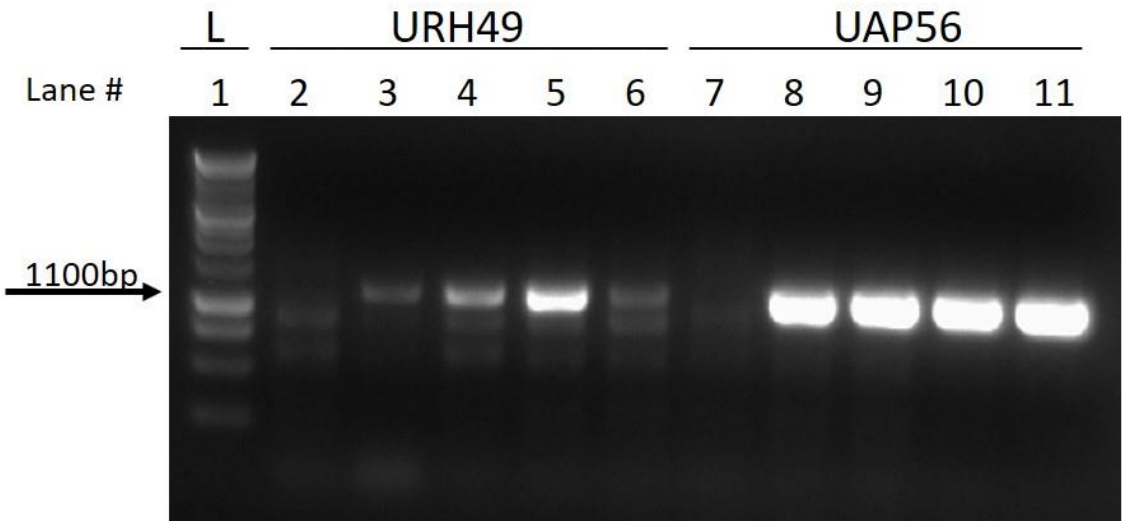

Figure 14 – *Second attempt PCR to amplify URH49 and UAP56 from GFP-positive population obtained through FACS* – Lanes 2-6: URH49 candidates 14-18. Lanes 7-11: UAP56 candidates 29-33. Amplified URH49 and UAP56 sequences were expected at 1100 base pairs. Amplification of URH49 sequences from candidates produced many non-specific bands while most UAP56 sequences were strongly amplified. We determined that there were too few cells obtained through FACS to give enough genomic DNA for amplification to occur.

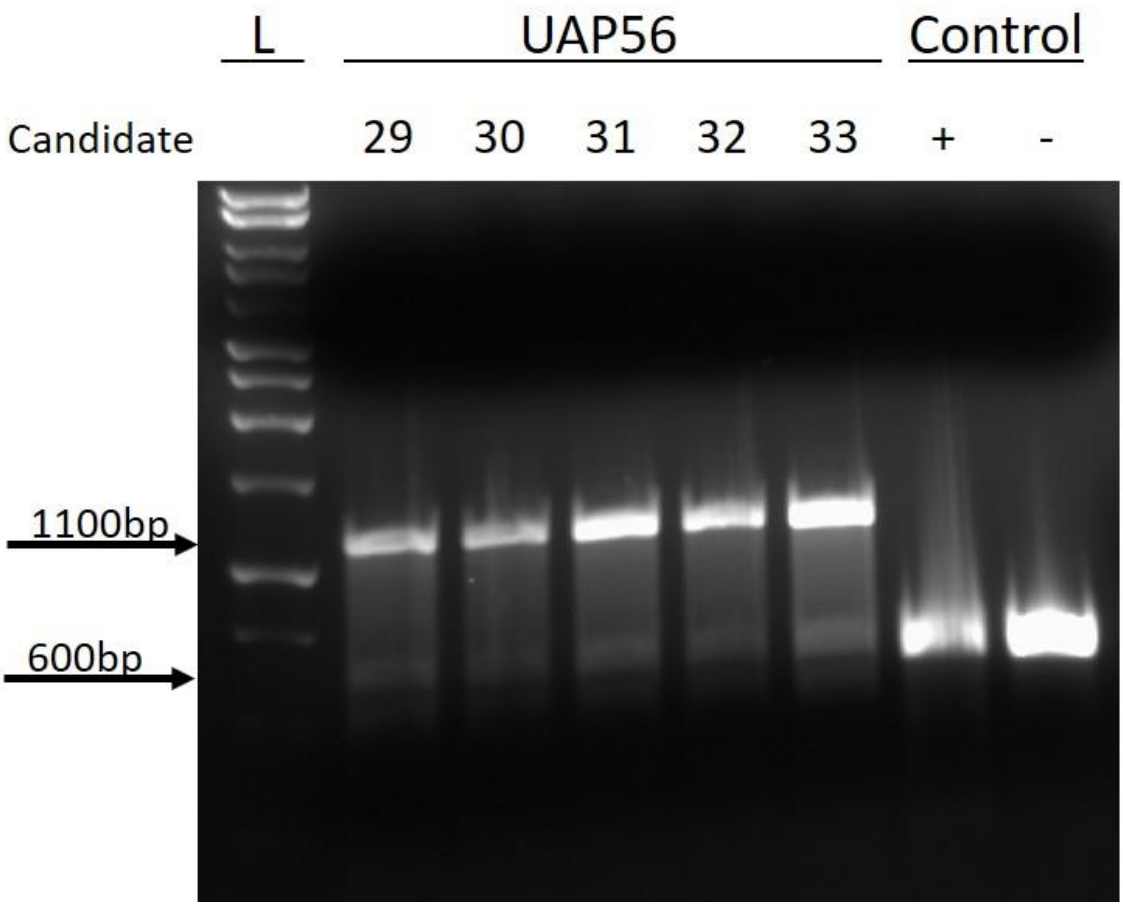

Figure 15 – *Surveyor nuclease assay of UAP56 plasmid candidates* – PCR product from candidates was hybridized with product from untreated control cells and treated with Surveyor nuclease. Surveyor treatment did not appear to cut the positive control and UAP56 candidates had degradation at approximately 600 base pairs.

Conclusions

Surveyor activity is clearly visible in control samples (figure 2), demonstrating its ability to discern the presence of mismatched bases in DNA. However, a mismatch is not likely to be observed if it is present in low abundance, an issue we observed when working with genomic DNA from a population of cells where transfection efficiency is low. This problem prompted the use of FACS to obtain a pure population of GFP-positive cells.

Ultimately, sorting CRISPR-transfected cells through FACS did not yield enough GFP-positive cells to determine if CRISPR was active and effectively targeting the genes of interest. Analysis of sort data using FSC-A vs. SSC-A, FSC-A vs. FSC-H, and PCA revealed transfection efficiencies as low as 0.9% and no higher than 4.1%.

PCR using genomic DNA extracted from these GFP-positive populations and analysis with Surveyor nuclease did not yield definitive results. While we did not detect surveyor endonuclease activity on our samples, the positive control in that trial did not work, leaving our data uninterpretable. Unfortunately, we did not recover enough DNA to repeat. Given the lack of promising data regarding the effectiveness of the CRISPR plasmids, we decided to employ a method utilizing small interfering RNAs (siRNAs) to assess the impact of UAP56, URH49, and export factor knockdown on viral replication.

CHAPTER FOUR

SMALL INTERFERING RNA

Background

RNA interference is a proven method to downregulate target gene expression. Indeed, there are commercially available small interfering RNAs guaranteed to target specific host genes with no off-target effects. We purchased SMART-pool siRNAs to evaluate the effect of knockdown of various host factors including the RNA helicases UAP56 and URH49, and the nuclear export factors Xpo5 and XpoT on viral RNA expression.

Export Factor Knockdown

Since influenza vRNPs express and replicate the genome in the nucleus, we were interested in the role of nuclear export factors in viral replication. Nxf1 is essential for successful influenza infection, as siRNA inhibition results in cell death and little infection (Larsen). Partial inhibition of Nxf1 did allow for permissive influenza infection and demonstrated that some, but not all, influenza mRNAs export from the nucleus via Nxf1 (Larsen et. al). Crm1 on the other hand is not involved in influenza mRNA nuclear export (Larsen) but is required for vRNP nuclear export during virion assembly (Neumann et al., 2000). Little is known regarding the possible role of additional host export factors Xpo5 and

XpoT. We aimed to determine if inhibition of these factors might inhibit viral replication.

In both A549 and Vero cells, XpoT and Xpo5 siRNAs were used to knock down their respective targets. In A549 cells (figure 16), knockdown is both robust and specific, reducing expression to less than 10% of normal. Expression of NP and PA was assessed and there was no significant change in the expression of either of these viral RNAs in either knockdown.

In Vero cells, Xpo5 and XpoT knockdown was specific and resulted in expression of less than 20% of normal (figure 17). Again, expression NP and PA was assessed and there was no significant change in the expression of either of the viral RNAs in either knockdown.

We can conclude from these data that Xpo5 and XpoT do not appear to have any significant impact on viral RNA expression at early timepoints of infection (within 4 hours post-infection).

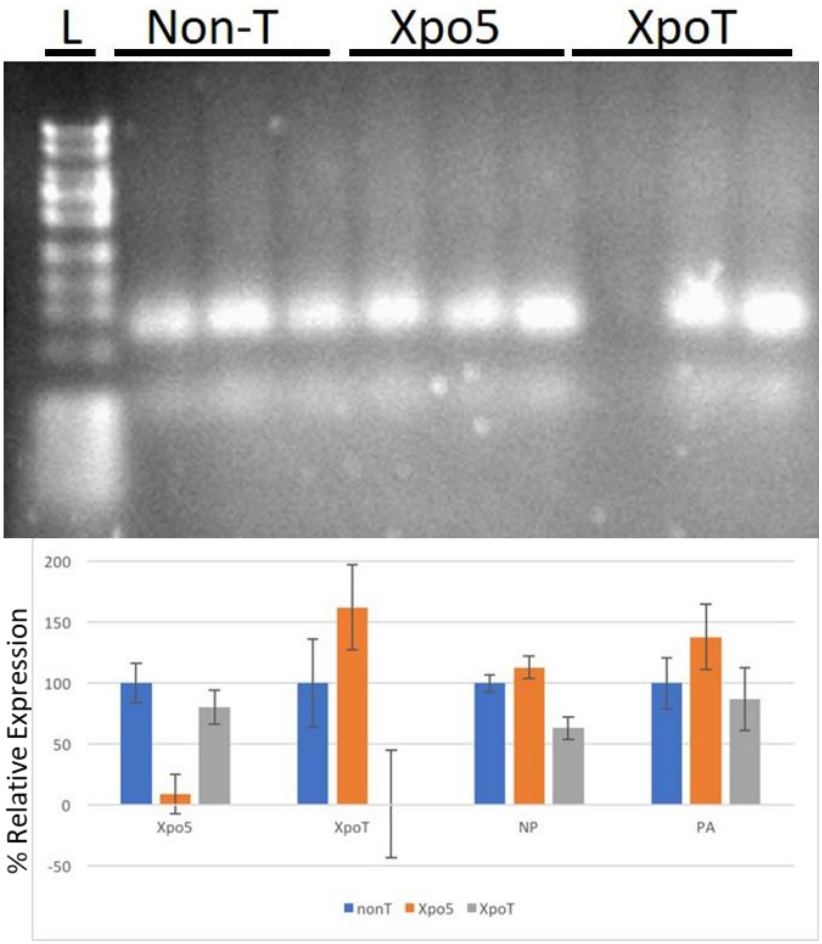

Figure 16 – *siRNA targeting Xpo5 and XpoT and Influenza infection in A549 cells, with Pedro Medina* – A. RNA was resolved on 1% bleach/agarose gel to ensure equal concentration and integrity. Two trials were selected for each sample to analyze in triplicate by RT-qPCR. Xpo5 and XpoT siRNA effectively knocked down their respective targets. There were no significant differences in NP or PA expression when either of these factors were knocked down, suggesting that they do not play an important role early during infection. Data obtained is from duplicate trials. Significance was determined with Student's Test using $P < 0.05$.

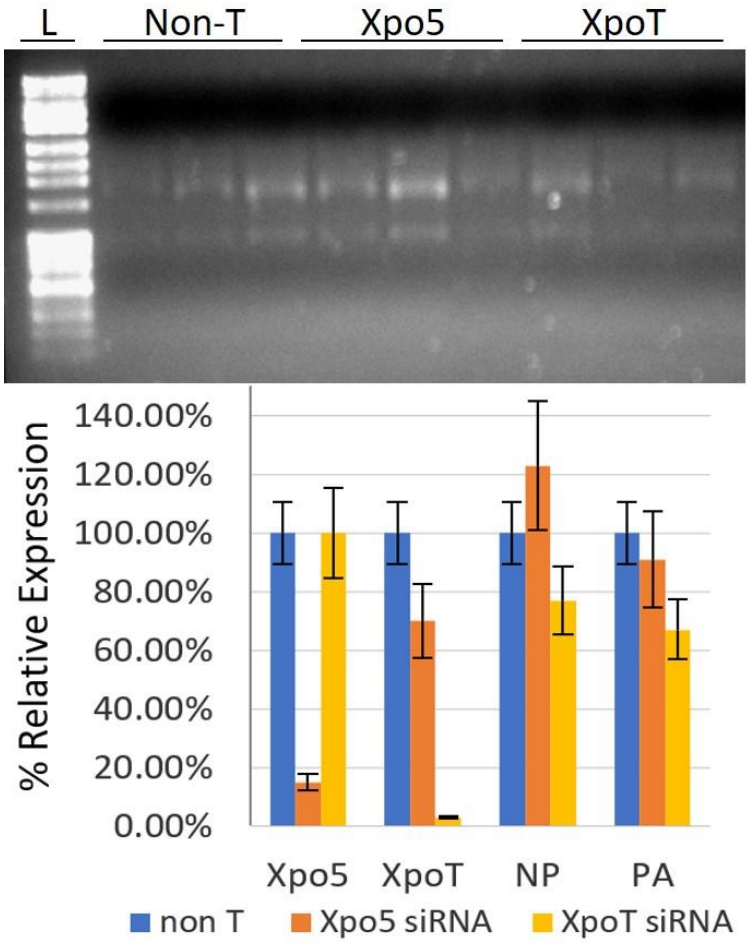

Figure 17 – *siRNA targeting Xpo5 and XpoT and Influenza infection in Vero cells, with Pedro Medina* – RNA was resolved on 1% bleach/agarose gel to ensure equal concentration and integrity. Two trials were selected for each sample to analyze in triplicate by RT-qPCR RNA as indicated was subject to RT-qPCR as indicated. Target siRNA results in Xpo5 expression at 15% of normal and XpoT expression reduced to 3% of normal. No cross-reactivity of siRNA was observed. There was no significant effect of Xpo5 or XpoT knockdown on influenza RNA expression of NP or PA. Data obtained is from duplicate trials. Significance was determined with Student's T-Test and $P < 0.05$.

UAP56 and URH49 Knockdown

UAP56 and URH49 have been implicated in separate studies to interact with the viral nucleoprotein (NP) and enhance viral RNA synthesis (Kawaguchi; Wisskerchen). Interestingly, only UAP56, and not URH49, was shown involved in unwinding dsRNA to limit the host innate interferon response (Wisskerchen). Our goal was to clarify the roles of these host factors and determine if either could serve as an antiviral target and inhibit influenza replication without harming self.

A549 cells were transfected with siRNA against UAP56 or DDX39, targeting both DEAD-box helicases URH49 and UAP56, also known as DDX39A and DDX39B, respectively. At 48 hours post transfection, cells were infected with Influenza A at a high multiplicity of infection to observe effect of host knockdown on a single infection cycle. We aim to inhibit an early stage of viral RNA replication and therefore isolated RNA at 4 hours post infection to assess viral RNA expression. RNA concentration was taken and equal concentration resolved on 1% agarose bleach gel (Figure 18). Reverse transcription followed by quantitative PCR confirms target knockdown for UAP56 and both UAP56 and URH49 when DDX39 siRNA is used. UAP56 was successfully knocked-down in only one trial, revealing a decrease in viral NP RNA expression, at about 25% of non-target siRNA treated control cells. Interestingly, UAP56 inhibition resulted in a concomitant URH49 increase. Inhibition of both UAP56 and URH49 also results in severe reduction in viral RNA expression. NP and PA RNA were

reduced to about 20% compared to non-target siRNA treated control cells and depending on how well URH49 was inhibited (Figure 18 and data not shown).

To determine if inhibition is due to UAP56's reported unwinding of dsRNA products, resulting in decreased host antiviral interferon response to improve viral replication, we repeated the siRNA analysis in VERO cells, which lack interferon. Similar to A549 cells, we see a decrease in both NP and PA expression when DDX39 is inhibited (figure 19). However, we did not detect expression of UAP56 in the non-target treated VERO cells, and therefore did not see reduction in expression when siRNA against UAP56 was transfected. We conclude the host factors have an interferon-independent effect on viral RNA expression. Further, we speculate VERO cells may rely more heavily on URH49 as UAP56 expression was not detected.

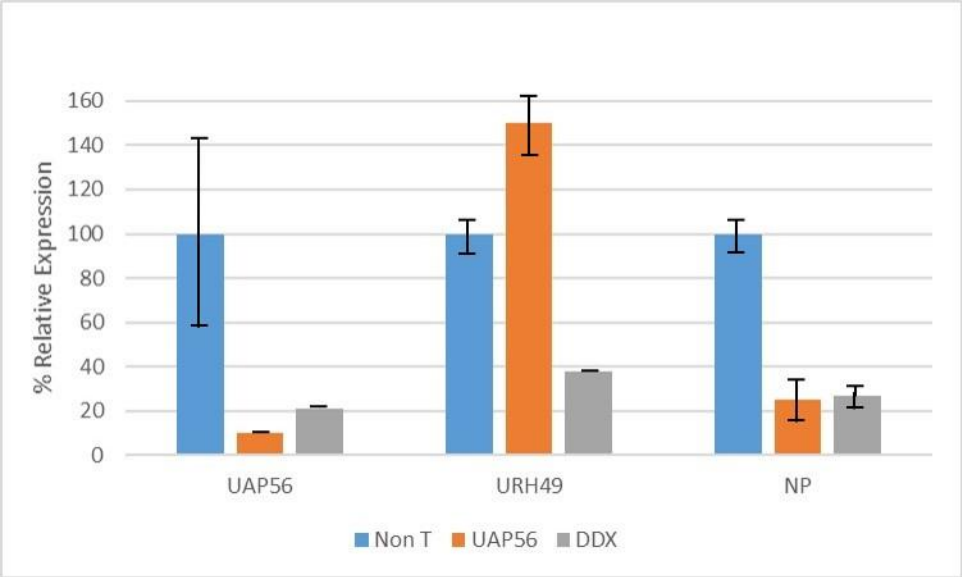

Figure 18 – *siRNA targeting UAP56 and DDX39 and Influenza infection in A549 cells.* – General DDX39 siRNA significantly reduced the expression of UAP56 and URH49. UAP56 siRNA was specific and also significantly reduced expression of its target. UAP56 siRNA caused a significant increase in URH49 expression to 150% of normal. Knockdown of UAP56 and URH49 resulted in significantly reduced expression of NP viral RNA. Results shown are qPCR triplicate data from one trial. Significance was determined with Student's T-Test and $P < 0.05$. RNA integrity data not shown.

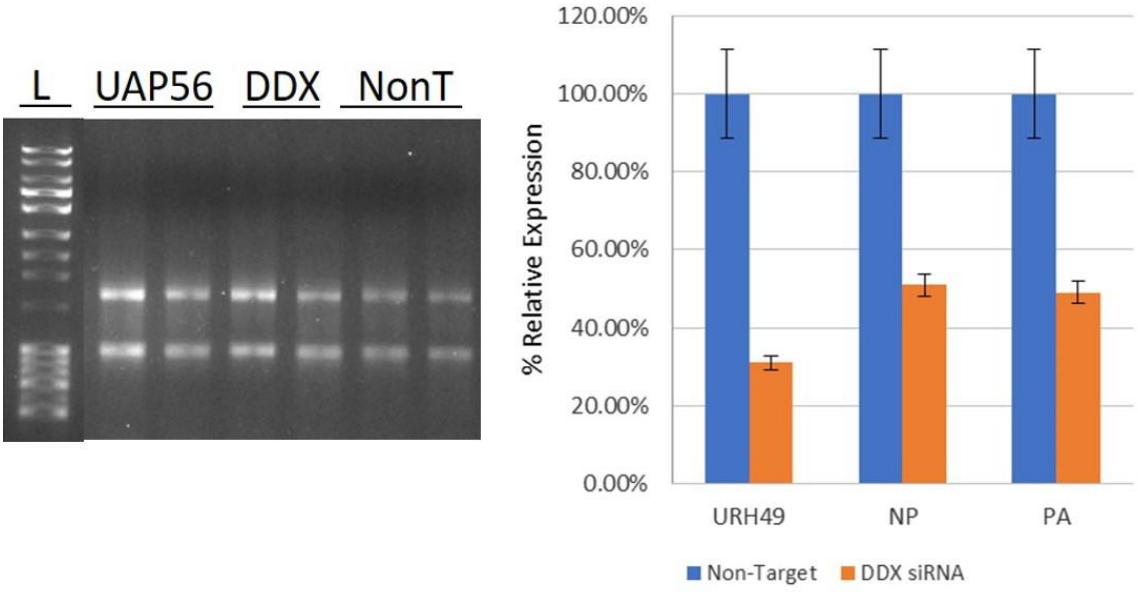

Figure 19 – *siRNA targeting DDX39 and Influenza infection in Vero cells* – RNA was resolved on 1% bleach/agarose gel to ensure equal concentration and integrity. DDX39 siRNA successfully knocked down expression of URH49 to 30% of normal. UAP56 was not detected above no RT control in VERO cells. DDX39 siRNA significantly reduced NP and PA expression. Significance was determined using Student's T-Test with $P < 0.05$.

Viability Assay

To determine whether UAP56 or URH49 could be reasonable targets within the host to combat Influenza infection, a viability assay was conducted to assess the toxicity of downregulation of UAP56 or UAP56 and URH49 in A549 cells. Cells transfected with siRNA were observed under the microscope at 48 hours post transfection. Nxf1 siRNA was previously observed to cause a high degree of cell death, and served as control for a highly toxic treatment. Conversely, non-targeted siRNA should only demonstrate toxicity caused by the transfection reagent and served as the healthy control.

As expected, cells incubated with Nxf1 siRNA displayed a high degree of cell death. At times, cellular debris obscures more than 50% of the visual field (figure 20, panel A-C). UAP56 siRNA-treated cells have similar cell death compared to non-target control based on microscopy images (panel D-F). DDX39 siRNA-treated cells (panel G-I) appeared to have similar, perhaps slightly more, cell death compared to UAP56 and the non-target control (panel J-L). Overall, based on the visual inspection, UAP56 knockdown appears to be relatively non-toxic.

Trypan blue exclusion was attempted to determine the percent live count of cells as a measure of toxicity between the samples. This analysis revealed great variability between triplicates and the data contradicted the visual microscopy assessment, indicating the non-target treated cells had the most cell death (Figure x). Based on our analysis we conclude that while inhibition of these

RNA helicases inhibits viral RNA expression, we do not observe massive cell death as seen with targeting an essential host factor such as Nxf1.

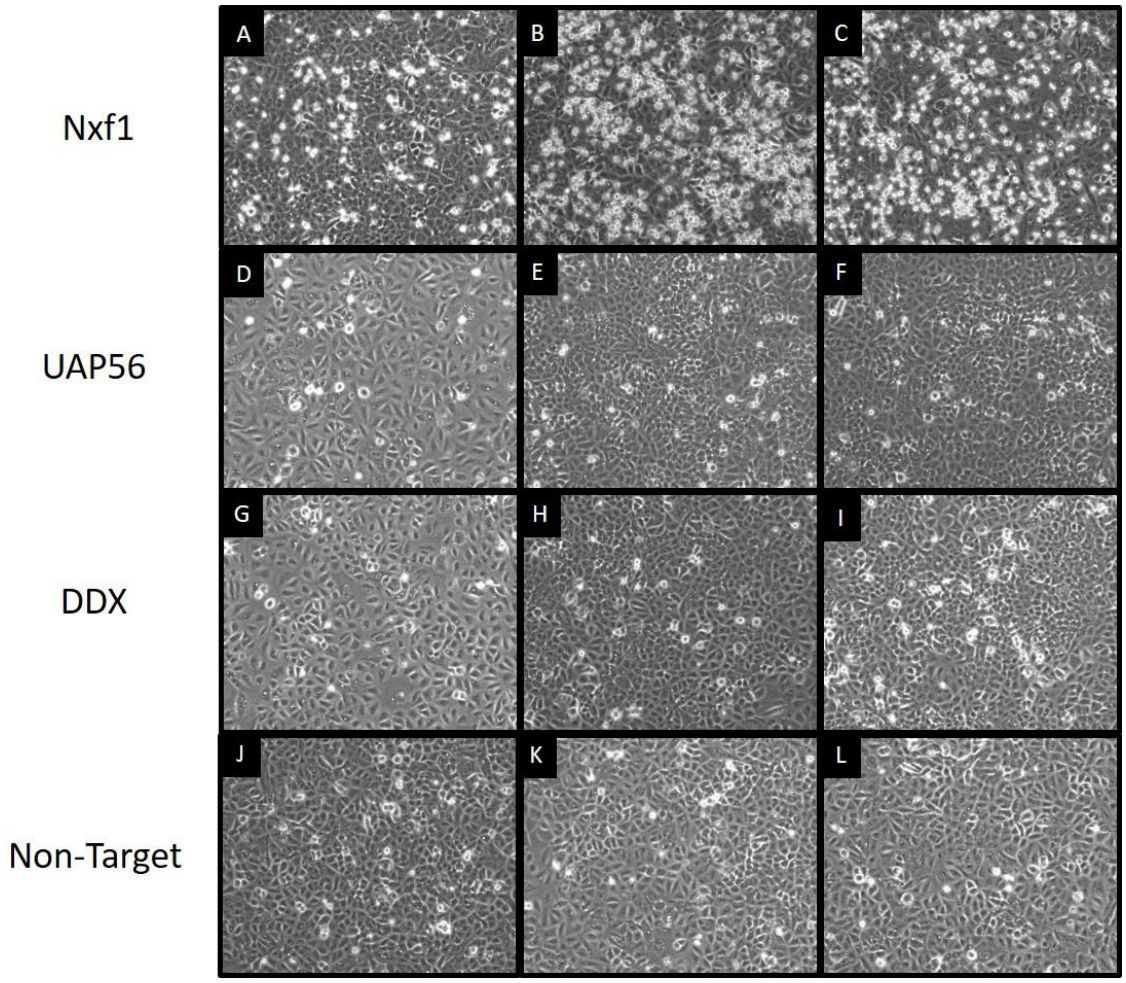

Figure 20 – *Visual assessment of siRNA-treated A549 cells* – Panel A-C: Nxf1 siRNA, control for high degree of cell death. Panel D-F: UAP56 siRNA. Panel G-I: DDX39 siRNA. Panel J-L: non-target siRNA, control for baseline cell death due to transfection reagent.

Conclusions

RNA interference allowed us to inhibit host factors and examine the effect on influenza viral RNA expression. From our results, we conclude neither Xpo5 nor XpoT contribute to viral RNA expression at early time points. There is no significant change in viral RNA expression when either of these factors is targeted. However, our data does supporting a role for host RNA helicases UAP56 and URH49 for optimal viral RNA expression. Targeted knockdown of UAP56 and URH49 results in reduced viral RNA expression in both A549 and VERO cells, indicating these factors play an interferon-independent role in viral RNA expression.

To determine if these factors are essential to the host cell, we used visual microscopy to assess A549 cells 48 hours post transfection with targeted siRNAs. Cells display a high degree of cell death when treated with Nxf1 siRNA. UAP56 and DDX39 siRNAs produce little to no additional toxicity compared to the non-targeted control. This suggests that targeted inhibition of UAP56 or URH49 may prove to be a relatively non-toxic treatment to combat Influenza infection. Consistent with redundant roles for these host factors, our results with VERO cells suggest they do not even express UAP56.

While it would have been preferable to collect quantitative data on cell viability, the assay encountered a major problem: the live counts associated with our highly-toxic control siRNA (Nxf1) had the highest percent-live counts while the non-toxic non-target control had the lowest percent live counts. I theorize that

the transfection reagent could be at fault here. Transfection reagent tends to have a low level of toxicity, but this toxicity may cause the cells to less-effectively efflux the trypan blue dye (whether due to faster penetration of the dye through the plasma membrane or by slower activity of efflux pumps) and appear to be “dead” to cell counters. Therefore, vital assays on cells subjected to transfection reagent as a means to introduce RNA or plasmids may require a method that does not rely on dyes in order to more-accurately discern live versus dead cells.

CHAPTER FIVE

CONCLUSIONS AND FUTURE DIRECTIONS

Summary

Influenza A is a highly pathogenic, negative-sense, single-stranded RNA virus of the *Orthomyxoviridae* family that is the causative agent of seasonal and pandemic flu. Vaccination, while highly effective in protecting against other disease-causing agents, is relatively ineffective and inconsistent in its protective capabilities due to the high degree of mutation associated with the inherent low fidelity of RNA polymerases and the virus' ability to re-assort. Additionally, antiviral treatments for Influenza infection are likely to become ineffective due to the development of resistance. In fact, resistance has already been observed. This means that developing new treatments for Influenza infections will be crucial for public health until a universal vaccine is developed.

Previous studies have implicated UAP56 and URH49, host RNA helicases, in viral replication. While they likely serve primarily redundant functions in the host, they are reported to have varied functions during viral infection. Here we demonstrate they have IFN independent effects on viral RNA expression; in particular, if both are inhibited, there is significant impact on viral RNA expression. While UAP56 is thought to be important for host mRNA export, we see no significant cell death 48 hours post transfection with siRNA inhibiting UAP56 or UAP56 and URH49, suggesting there may be additional DEAD-Box

RNA helicases that can function as DDX39. It is this redundancy of function in the host but centrality for viral replication that makes UAP56 and URH49 prime targets for development of a novel antiviral therapy.

While CRISPR did not yield cell lines null for UAP56 or URH49, siRNA studies found several important things about the role of these RNA helicases in Influenza viral RNA expression. Knockdown of host RNA helicases UAP56 or DDX39 (UAP56 and URH49) provided additional evidence to support a role for UAP56 and URH49 to enhance viral RNA expression. We found that these RNA helicases are important for viral RNA expression even in the absence of a host IFN response, as observed in Vero cells.

Visual assessment of cell death over three separate trials indicated that UAP56 siRNA treatment was similar to the relatively non-toxic non-targeted treatment. This provides some evidence that UAP56 may indeed be a viable target for novel antiviral therapy.

Given that influenza virus replicates in the nucleus, we also analyzed the effect of inhibiting host nuclear export factors prior to influenza infection. Our results here revealed that inhibition of Xpo5 (miRNA export) or XpoT (tRNA export) in either A549 or Vero cells has no significant effect on viral NP and PA expression. Targeted knockdown of these factors did not cause any significant change in viral RNA synthesis at early stage of the viral lifecycle. Therefore, these host factors are not as promising targets for development of novel antiviral therapies as the DDX39 helicases.

Future Directions

While CRISPR attempts did not generate a null cell line, it may be possible for future work to be done in commercially available knockout cell lines already established as knockout of UAP56 or URH49. While siRNA has shown to be effective in knocking down gene expression of specific targets, knock down can be inconsistent and range from near complete knockdown to only 25% knockdown of the same target depending on experiment (for example, see chapter 4: figures 16 and 19). Purchasing a knockout cell line would eliminate much of the variability from the method.

While Nxf1 plays a major role during influenza infection, it is also an essential host factor and as such would not be a good target for novel antivirals. Analysis of the additional members of the Nxf group of export factors, including Nxf2, Nxf3, Nxf4, and Nxf5, may reveal novel roles and activities for these host factors and may define them as possible host targets to inhibit viral replication.

WORKS CITED

Scholarly Journals

Barrangou R, Fremaux C, Deveau H, Richards M, Boyaval P, Moineau S, Romero DA, Horvath P. 2007. CRISPR Provides Acquired Resistance Against Viruses in Prokaryotes. Science 315:1709–1712.

Bouvier NM, Palese, P. 2008. THE BIOLOGY OF INFLUENZA VIRUSES. Vaccine 12(26):D49–D53.

Carmody S, Wente S. 2009. mRNA nuclear export at a glance. Journal of Cell Science, 12:1933–1937.

CDC Estimates of 2009 H1N1 Influenza Cases, Hospitalizations and Deaths in the United States. June 24, 2014. Atlanta (GA): Center for Disease Control; [accessed 2016 Aug 21]. https://www.cdc.gov/h1n1flu/estimates_2009_h1n1.htm

Coleman J R. 2007. The PB1-F2 protein of Influenza A virus: increasing pathogenicity by disrupting alveolar macrophages. Virology Journal 4(9).

Cong L, Ran FA, Cox D, Lin S, Barretto R, Habib N, HSU PD, Wu X, Jiang W, Zhang, F. 2013. Multiplex Genome Engineering Using CRISPR/Cas Systems. Science 339:819–823.

Elton D, Simpson-Holley M, Archer K, Medcalf L, Hallam R, McCauley J, Digard, P. 2001. Interaction of the Influenza Virus Nucleoprotein with the Cellular CRM1-Mediated Nuclear Export Pathway. Journal of Virology 75(1):408–419.

Fleckner, J, Zhang M, Valcarcel J, Green MR. 1997. U2AF65 recruits a novel human DEAD box protein required for the U2 snRNP-branchpoint interaction. Genes and Development 11:1864–1872.

Hale BG, Randall RE, Ortin J, Jackson D. 2008. The multifunctional NS1 protein of influenza A viruses. Journal of General Virology 89:2359–2376.

Hutchinson EC, Hodor E. 2013. Transport of the Influenza Virus Genome from Nucleus to Nucleus. Viruses 5:2424–2446.

Jarmoskaite I, Russell R. 2011. DEAD-box proteins as RNA helicases and chaperones. Wiley Interdisciplinary Reviews 2(1):135–152.

Kawaguchi A, Momose F, Nagata K. (2011). Replication-Coupled and Host Factor-Mediated Encapsidation of the Influenza Virus Genome by Viral Nucleoprotein. Journal of Virology 85(13):6197–6204.

Larsen S, Bui S, Perez V, Mohammad A, Medina-Ramirez H, Newcomb LL. 2014. Influenza polymerase encoding mRNAs utilize atypical mRNA nuclear export. Virology Journal 11(154).

Levasseur A, Mekliz M, Chabriere E, Pontarotti P, La Scola B, Raoult D. 2016. MIMIVIRE is a defence system in mimivirus that confers resistance to virophage. Nature 531:249–252.

Molinari N, Ortega-Sanchez I, Messonnier M, Thompson W, Wortley P, Weintraub E, Bridges C. 2007. The annual impact of seasonal influenza in the US: measuring disease burden and costs. Vaccine 25(27):5086–5096.

Momose F, Basler C, O'Neill R, Iwamatsu A, Palese P, Nagata K. 2001. Cellular splicing factor RAF-2p48/NPI-5/BAT1/UAP56 interacts with the influenza virus nucleoprotein and enhances viral RNA synthesis. Journal of Virology 75(4):1899–1908.

Neumann G, Hughes M T, Kawaoka, Y. 2000. Momose, F., Basler, C., O'Neill, R., Iwamatsu, A., Palese, P., & Nagata, K. (2001). Cellular splicing factor RAF-2p48/NPI-5/BAT1/UAP56 interacts with the influenza virus nucleoprotein and enhances viral RNA synthesis. Journal of Virology 75(4):1899–1908.

Okamura M, Inose H, Masuda S. 2015. RNA Export through the NPC in Eukaryotes. Genes 6:124–149.

O'Neill RE, Talon J, Palese P. 1998. The influenza virus NEP (NS2 protein) mediates the nuclear export of viral ribonucleoproteins. The EMBO Journal 17(1):288–296.

Paterson D, Fodor E. 2012. Emerging Roles for the Influenza A Virus Nuclear Export Protein (NEP). PLOS Pathogens 8(12):1-8.

Thomas M, Lischka P, Muller R, Stamminger T. 2011. The Cellular DExD/H-Box RNA-Helicases UAP56 and URH49 Exhibit a CRM1-Independent Nucleocytoplasmic Shuttling Activity. PLOS One 9(7):1-14.

Wilson R C, Doudna JA. 2013. Molecular Mechanisms of RNA Interference. Annual Review of Biophysics 42:217–239.

Wisskirchen C, Ludersdorfer TH, Mueller DA, Mortiz E, Pavlovic J. 2011. The Cellular RNA Helicase UAP56 Is Required for Prevention of Double-Stranded

RNA Formation during Influenza A Virus Infection. Journal of Virology 85(17):8646–8655.

Online Resources

Bionumbers. November 20, 2010. Cambridge (MA): Harvard University; [accessed 2016 Mar 23]. http://bionumbers.hms.harvard.edu/bionumber.aspx?id=101605&ver=10

CDC Estimates of 2009 H1N1 Influenza Cases, Hospitalizations and Deaths in the United States. June 24, 2014. Atlanta (GA): Center for Disease Control; [accessed 2016 Aug 21]. https://www.cdc.gov/h1n1flu/estimates_2009_h1n1.htm

Epidemiology and Prevention of Vaccine-Preventable Diseases, Chapter 12: Influenza. November 15, 2016. Atlanta (GA): Centers for Disease Control; [accessed 2017 Oct 16]. https://www.cdc.gov/vaccines/pubs/pinkbook/flu.html

Influenza. March, 2003. Geneva (Switzerland); [accessed 2018 Mar 23]. http://www.who.int/mediacentre/factsheets/2003/fs211/en/

Influenza Type A Viruses. April 19, 2016. Atlanta (GA): Centers for Disease Control; [accessed 2017 Oct 15]. https://www.cdc.gov/flu/avianflu/influenza-a-virus-subtypes.htm

Key Facts About Seasonal Flu Vaccine. October 30, 2017. Atlanta (GA): Centers for Disease Control; [accessed 2018 Feb 10]. https://www.cdc.gov/flu/protect/keyfacts.htm

Seasonal Influenza Vaccine Effectiveness. February 15, 2018. Atlanta (GA): Centers for Disease Control; [accessed 2018 Mar 23]. https://www.cdc.gov/flu/professionals/vaccination/effectiveness-studies.htm

What You Should Know About Flu Antiviral Drugs. January 23, 2018. Atlanta (GA): Centers for Disease Control; [accessed 2018 Mar 23]. https://www.cdc.gov/flu/antivirals/whatyoushould.htm